Supplementary Information (SI) for Chemical Communications.
This journal is © The Royal Society of Chemistry 2024

Electronic Supplementary Information

Photoactivable Malachite Green-Based Alkynylplatinum(II) 2,6-Bis(*N*-alkylbenzimidazol-2-yl)pyridine Complexes

Andy Shun-Hoi Cheung, Ming-Yi Leung, Tony Ho-Ching Fung and Vivian Wing-Wah Yam*

Institute of Molecular Functional Materials and Department of Chemistry, The University of Hong Kong, Pokfulam Road, Hong Kong, P. R. China

*Corresponding author: wwyam@hku.hk

Experimental

Materials and Reagents

Acetonitrile (MeCN) (ACS spectrophotometric grade) was purchased from Sigma-Aldrich Co. Ltd. [D_6]-Acetone and [D_3]-acetonitrile were purchased from Cambridge Isotope Laboratories, Inc. Tetra-*n*-butylammonium fluoride solution (1.0 M in THF) was purchased from J & K Scientific Ltd. 4,4′-bis(dimethylamino)-benzophenone and 1,7-octadiyne were purchased from Sigma-Aldrich Chemcial Co. ((4-Bromophenyl)ethynyl)tri-*iso*-propylsilane[1] and 1,8-bis(4-bromophenyl)octa-1,7-diyne[2] were synthesized and purified according to the procedures reported previously. All other commercially available reagents were of analytical grade and were used as received. All solvents were purified by the Innovative Technology, Inc. PureSolv MD 5 Solvent Purification System before use. All amines were distilled over sodium hydroxide and stored over sodium hydroxide before use. All reactions were performed under inert and anhydrous conditions using standard Schlenk techniques unless specified otherwise.

Caution: *The synthesis of malachite green derivatives involved the use of potassium cyanide which is highly toxic and should be handled with great caution. The excess and/or residue potassium cyanide should be quenched by excess aqueous ammonium iron(II) sulphate solution. The formation of a dark blue precipitate, which is the Prussian Blue, would indicate the complete quenching of potassium cyanide. Also, any acid and/or acidic vapour should be avoided when performing the reaction in the fumehood, including both the setting up and working up processes.*

Physical Measurements and Instrumentation

^{1}H NMR spectra were recorded on a Bruker AVANCE 300 (300 MHz) or a Bruker AVANCE 500 (500 MHz) NMR spectrometers with chemical shifts relative to tetramethylsilane (Me_4Si). Electron impact (EI) mass spectra were recorded on a Thermo Scientific DFS High Resolution Magnetic Sector mass spectrometer. High-resolution electrospray ionization (ESI) mass spectra were recorded on a Bruker maXisII high-resolution LC-QTOF mass spectrometer. All elemental analyses were performed on a Flash EA 1112 elemental analyser by the Institute of Chemistry at the Chinese Academy of Sciences in Beijing. IR spectra were obtained in the solution state on a IRAffinity-1 Fourier transform infrared spectrophotometer (4000–500 cm^{-1}). UV–Visible absorption spectra were obtained by using a Varian Cary 50 UV/Vis spectrophotometer. Photoirradiation was performed using a UVGO 254-nm 12 W UVC LED lamp. The UV–visible spectral changes upon UV irradiation was monitored by an Agilent Cary 8454 diode array spectrophotometer. Transmission electron microscopy (TEM) experiments were performed on a Philips CM100 transmission electron microscope. Scanning electron microscopy (SEM) experiments were performed on a Leo 1530 Field-Emission-Gun scanning electron microscope. The selected area electron diffraction (SAED) experiments were performed on a FEI Tecnai G2 20 S-TWIN transmission electron microscope with an accelerating voltage of 200 kV. All carbon-coated copper grids were pre-treated with a PELCO easiGlow Glow Discharge Cleaning System. Samples were prepared by dropping a few drops of sample solution onto the grids and dried by slow evaporation of the solvents. X-Ray diffraction data were collected on Bruker D8 ADVANCE Powder X-ray Diffractometer in Bragg-Brentano ($\theta/2\theta$) reflection mode with a graphite monochromatized Cu-K_α radiation (λ = 1.54178 Å) and nickel filter.

Computational Details

Gaussian 09 software package[3] was adopted for the calculations. Density functional theory (DFT) with the M06 functional,[4] which is suggested for investigations of transition metal thermochemistry and for properly considering non-covalent interactions,[4,5] was used to optimize the ground state (S_0) geometries of the model complexes of **1** (**1′** and **1″**). **1′** and **1″** were investigated in conjunction with the solvation model density (SMD) continuum method[6] using acetonitrile (MeCN) as the solvent. On the basis of the optimized S_0 geometries, time-dependent DFT (TDDFT)[7–9] calculations at the same level associated with CPCM (MeCN) were performed to compute the singlet–singlet transitions. Non-Covalent Interactions (NCI) isosurfaces of the dimers of **1′** and **1″** were obtained with the NCIPLOT code,[10,11] which was based on the electron density and its gradient, and the results were visualized with the Visual Molecular Dynamic (VMD) program.[12] Vibrational frequencies were subsequently calculated at the same level of theory for the optimized geometries to verify that each was a minimum (NIMAG = 0) on the potential energy surface. The Stuttgart effective core potentials (ECPs) and the associated basis set were used to describe platinum[13] with two f-type polarization functions (ζ = 0.70 and 0.14),[14] whereas the 6-31G(d,p) basis set was employed to describe all other atoms.[15–17] The DFT calculations were performed with a pruned (99,590) grid for numerical integration.

The TDDFT calculations show that the low-energy absorption band at 453 nm corresponds to the HOMO−2→LUMO transition in **1′**. The HOMO−2 of **1′** corresponds to the π orbitals localized on the malachite green (MG) leucocyanide and the d-orbitals of the Pt(II) centre, while the LUMO of **1′** corresponds to the π^* orbitals localized on the bzimpy ligand. Therefore, the low-energy absorption band of **1′** can be assigned as the metal-to-ligand charge transfer (MLCT) [dπ(Pt)→π^*(bzimpy)] and ligand-to-ligand charge transfer (LLCT) [π(MG)→π^*(bzimpy)] transitions. These calculations are in line with the assignments in the electronic absorption study of **1**. On the other hand, the low-energy absorption band at 528 nm

in **1″** corresponds to the HOMO→LUMO transition. The HOMO of **1″** corresponds to the π orbitals mainly localized on the ionic form of MG moiety, while the LUMO corresponds to the π^* orbitals localized on the ionic form of MG moiety, and the alkynyl and bzimpy ligands. Therefore, the low-energy absorption band of **1″** can be assigned as the intraligand (IL) [π(MG)→π*(MG)] transition, with some mixing of ligand-to-ligand charge transfer (LLCT) [π(MG)→π*(bzimpy)] transitions. Due to the failure of obtaining the pure photoionized product of **1**, the results from the computational studies could not be directly compared. The first ten singlet (S_n) excited states of **1′** and **1″** have been computed with the TDDFT/CPCM (MeCN) method (Tables S2–S3). Selected frontier molecular orbitals of **1′** and **1″** as well as the simulated electronic absorption spectra based on the TDDFT results are summarized in Fig. S23–S25.

Synthetic Procedures

TIPS–C≡C–MG–CN (**L1**). It was prepared according to a modification of the procedure reported for the synthesis of 2,2′-bis(4-(dimethylamino)phenyl)-2-(4-(2-hydroxyethoxy)phenyl)acetonitrile,[18] except that ((4-bromophenyl)ethynyl) triisopropylsilane (1.68 g, 4.99 mmol) was used in place of 2-(4-bromophenoxy)ethanol. Yield: 0.681 g, 1.27 mmol; 25.5 %. ^{1}H NMR (300 MHz, [D$_6$]-acetone, 298 K, δ/ppm): δ 1.15 (s, 21H, –Si(CH(CH$_3$)$_2$)$_3$), 2.96 (s, 12H, –N–(CH$_3$)$_2$), 6.74 (d, J = 8.7 Hz, 4H, phenyl), 6.99 (d, J = 8.7 Hz, 4H, phenyl), 7.23 (d, J = 8.2 Hz, 2H, phenyl), 7.54 (d, J = 8.2 Hz, 2H, phenyl). HRMS (Positive ESI): calcd for C$_{35}$H$_{45}$N$_3$Si, *m/z* 536.3456; found: 536.3453 [M+H]$^+$.

Br–C$_6$H$_4$–(C≡C–(CH$_2$)$_4$–C≡C–MG–CN)-4 (**L2**). It was prepared according to a modification of the procedure reported for the synthesis of 2,2′-bis(4-(dimethylamino)phenyl)-2-(4-(2-hydroxyethoxy)phenyl)acetonitrile,[18] except that 1,8-bis(4-bromophenyl)octa-1,7-diyne (2.99 g, 7.18 mmol) was used in place of 2-(4-bromophenoxy)ethanol. Yield: 0.342 g, 0.556 mmol; 7.74 %.^{1}H NMR (300 MHz, [D$_6$]-acetone, 298 K, δ/ppm): δ 1.78 (s, 4H, –CH$_2$–), 2.50 (s, 4H, –CH$_2$–), 2.96 (s, 12H, –N–(CH$_3$)$_2$), 6.73 (d, J = 8.7 Hz, 4H, phenyl), 6.98 (d, J = 8.7 Hz, 4H, phenyl), 7.18 (d, J = 8.0 Hz, 2H, phenyl), 7.33 (d, J = 8.0 Hz, 2H, phenyl), 7.43 (d, J = 8.0 Hz, 2H, phenyl), 7.51 (d, J = 8.0 Hz, 2H, phenyl). HRMS (Positive EI): calcd for C$_{38}$H$_{36}$N$_3$Br, *m/z* 613.2165; found: 613.2097 [M]$^+$.

[Pt{bzimpy(C$_{10}$H$_{21}$)$_2$}{C≡C–MG–CN}]PF$_6$ (**1**). To a stirred solution of [Pt{bzimpy(C$_{10}$H$_{21}$)$_2$}Cl]PF$_6$ (150 mg, 0.155 mmol) and TIPS–C≡C–MG–CN (L1) (100 mg, 0.187 mmol) in dichloromethane (20 mL) was added a catalytic amount of copper(I) iodide (10 mg) and triethylamine (2 mL) at 0 °C. Subsequently, tetra-*n*-butylammonium fluoride (2 mL, excess) in THF solution was added slowly. The reaction was allowed to stir overnight. After removal of solvent, the crude product was purified by slow diffusion of diethyl ether vapor into

the concentrated dichloromethane solution to give the products of complex **1** as an orange solid. Yield: 85.1 mg, 0.0650 mmol; 41.9 %. ^{1}H NMR (500 MHz, [D$_6$]-acetone, 298 K, δ/ppm): δ 0.84 (t, J = 7.0 Hz, 6H, –CH$_3$), 1.23–1.28 (m, 24H, –CH$_2$–), 1.32–1.35 (m, 4H, –CH$_2$–), 1.48–1.51 (m, 4H, –CH$_2$–), 3.00 (s, 12H, –N–(CH$_3$)$_2$), 4.81–4.85 (m, 4H, –N–CH$_2$–), 6.82 (d, J = 8.8 Hz, 4H, phenyl), 7.10 (d, J = 8.8 Hz, 4H, phenyl), 7.33 (d, J = 8.5 Hz, 2H, benzimidazolyl), 7.59–7.63 (m, 4H, phenyl and benzimidazolyl), 7.69 (t, J = 7.5 Hz, 2H, benzimidazolyl), 7.77 (d, J = 8.5 Hz, 2H, phenyl), 8.53–8.59 (m, 3H, pyridine), 8.62 (d, J = 8.5 Hz, 2H, benzimidazolyl). HRMS (Positive ESI): calcd for C$_{65}$H$_{77}$N$_8$Pt, *m/z* 1165.5933; found: 1165.5923 [M–PF$_6$]$^+$. Elemental analysis calcd (%) for C$_{65}$H$_{77}$F$_6$N$_8$PPt•0.5CH$_2$Cl$_2$: C, 58.15; H, 5.81; N, 8.28; found: C, 58.37; H, 5.85; N, 8.59.

[Pt{bzimpy(C$_{10}$H$_{21}$)$_2$}{C≡C–C$_6$H$_4$–(C≡C–(CH$_2$)$_4$–C≡C–MG–CN)-4}]PF$_6$ (**2**). To a degassed solution of Br–C$_6$H$_4$–(C≡C–(CH$_2$)$_4$–C≡C–MG–CN)-4 (L2) (0.341 g, 0.554 mmol) in diisopropylamine (15 mL) was added [Pd(PPh$_3$)$_2$Cl$_2$] (100 mg, 0.142 mmol), copper(I) iodide (100 mg, 0.523 mmol) and (triisopropylsilyl)acetylene (2.10 mL, 9.36 mmol). The reactions mixture was allowed to reflux for 2 hours. After cooling to room temperature, the reaction mixture was filtered and the solvent was removed in vacuo. To the stirred solution of this crude product in dichloromethane (20 mL) was added [Pt{bzimpy(C$_{10}$H$_{21}$)$_2$}Cl]PF$_6$ (150 mg, 0.155 mmol), a catalytic amount of copper(I) iodide (10 mg) and triethylamine (2 mL) at 0 °C. Subsequently, tetra-*n*-butylammonium fluoride (2 mL, excess) in THF solution was added slowly. The reaction was allowed to stir overnight. After removal of solvent, the crude product was purified by slow diffusion of diethyl ether vapor into the concentrated dichloromethane solution to give the products of complex **2** as an orange solid. Yield: 38.3 mg, 0.0257 mmol; 16.6 %. ^{1}H NMR (500 MHz, [D$_6$]-acetone, 298 K, δ/ppm): δ 0.85 (t, J = 7.0 Hz, 6H, –CH$_3$), 1.24–1.30 (m, 24H, –CH$_2$–), 1.43–1.49 (m, 4H, –CH$_2$–), 1.86–1.87 (m, 4H, –CH$_2$–), 1.97–2.01 (m, 4H, –CH$_2$–), 2.58–2.61 (m, 4H, –CH$_2$–), 2.93 (s, 12H, –N–(CH$_3$)$_2$), 4.69–4.71

(m, 4H, –N–CH_2–), 6.72 (d, J = 8.5 Hz, 4H, phenyl), 6.98 (d, J = 8.5 Hz, 4H, phenyl), 7.21 (d, J = 8.0 Hz, 2H, phenyl), 7.43–7.51 (m, 6H, phenyl), 7.54 (t, J = 7.5 Hz, 2H, benzimidazolyl), 7.60 (t, J = 7.5 Hz, 2H, benzimidazolyl), 7.65 (d, J = 8.0 Hz, 2H, benzimidazolyl), 8.40–8.44 (m, 4H, benzimidazolyl and pyridine), 8.53 (t, J = 8.0 Hz, 1H, pyridine). HRMS (Positive ESI): calcd for $C_{79}H_{89}N_8Pt$, *m/z* 1345.6875; found: 1345.6849 $[M–PF_6]^+$. Elemental analysis calcd (%) for $C_{79}H_{89}F_6N_8PPt$: C, 63.65; H, 6.02; N, 7.52; found: C, 63.23; H, 6.00; N, 7.51.

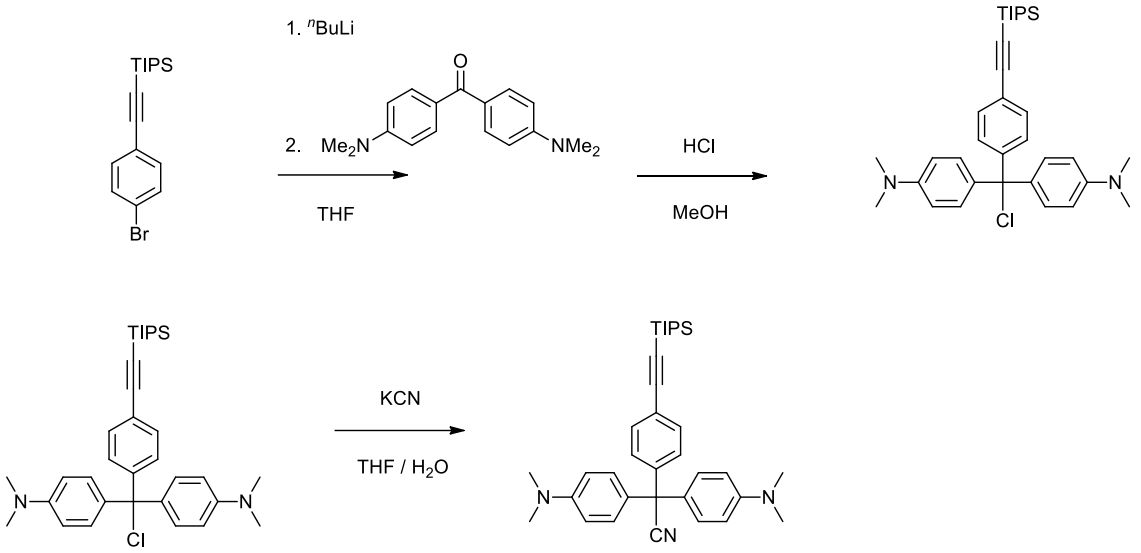

Scheme S1 Synthetic route for **L1**.

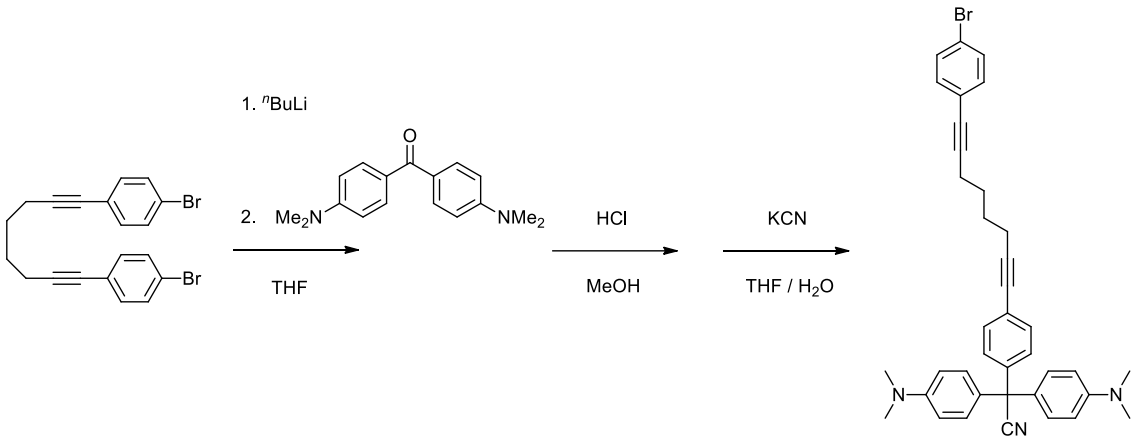

Scheme S2 Synthetic route for **L2**.

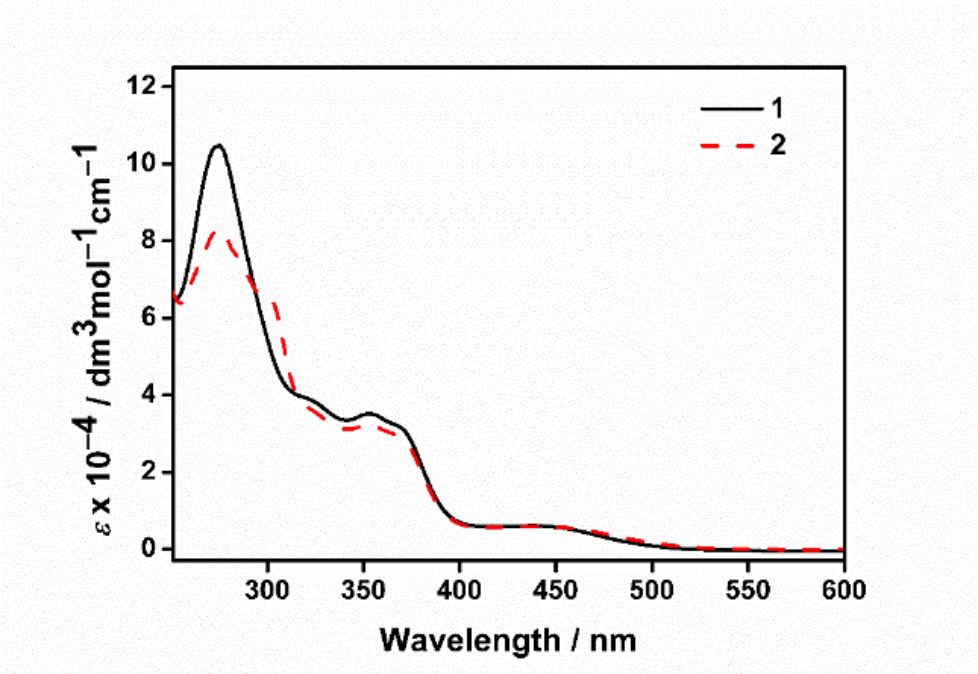

Fig. S1 Electronic absorption spectra of **1** and **2** in MeCN solutions at 298 K.

Table S1 Photophysical data of **1** and **2** in MeCN at 298 K

Complex	**Absorption**
	λ_{max} / nm (ε_{max} / $dm^3\ mol^{-1}\ cm^{-1}$)
1	275 (105000), 330sh (36300), 354 (35200), 370sh (31300), 452 (5670)
2	274 (83400), 305 (61300), 350 (32100), 454 (5720)

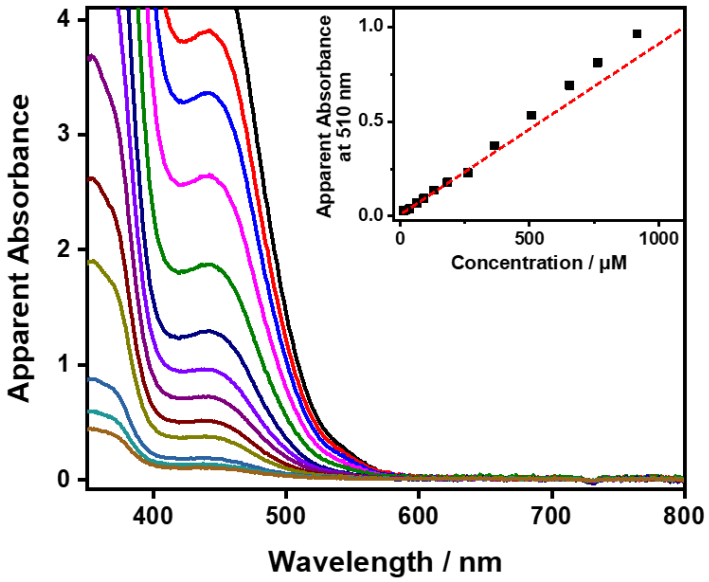

Fig. S2 Concentration-dependent UV–visible absorption spectra of **1** in MeCN in the concentration range of 9.15×10^{-4} to 1.30×10^{-5} M. Inset: Plot of apparent absorbance against concentration, monitored at 510 nm. The apparent absorbance values were obtained by correcting to 1-cm pathlength equivalence.

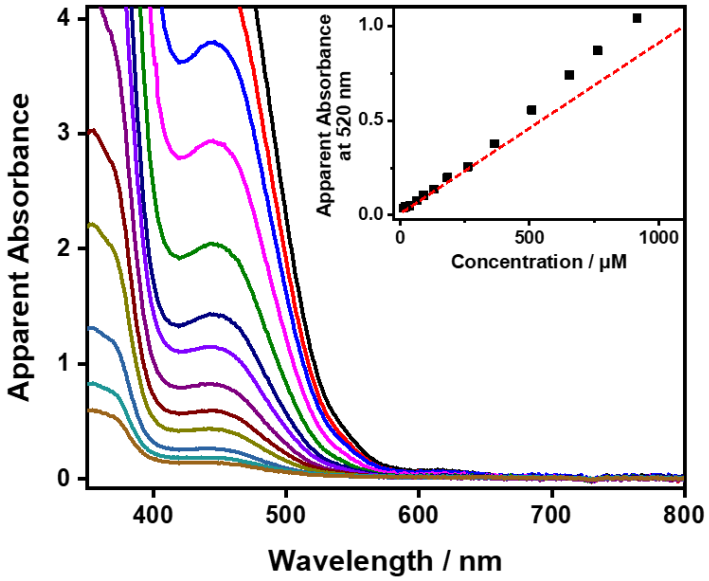

Fig. S3 Concentration-dependent UV–visible absorption spectra of **2** in MeCN in the concentration range of 8.99×10^{-4} to 1.28×10^{-5} M. Inset: Plot of apparent absorbance against concentration, monitored at 520 nm. The apparent absorbance values were obtained by correcting to 1-cm pathlength equivalence.

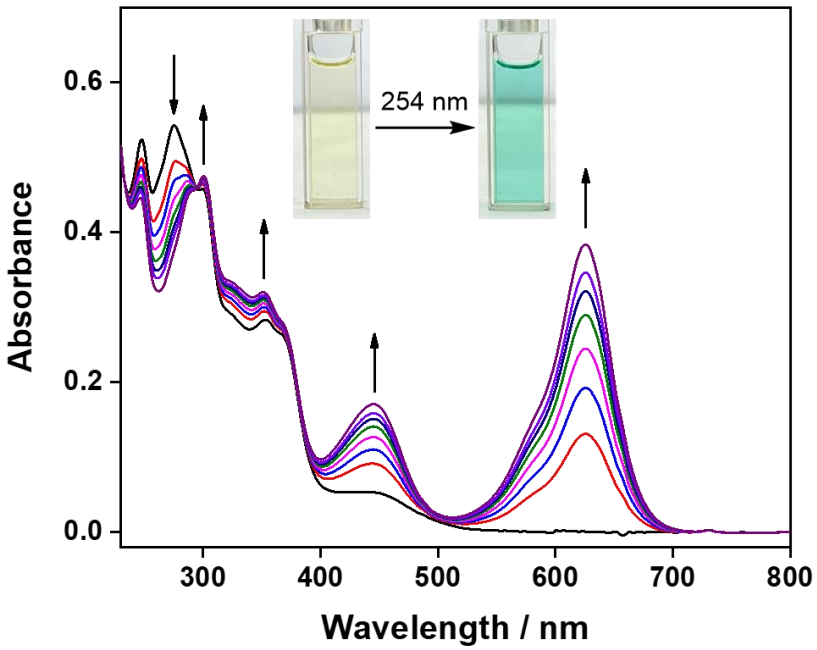

Fig. S4 UV–Visible spectral changes of **2** in MeCN upon photo-irradiation at 254 nm ([**2**] = 8.73×10^{-6} M). Spectra were taken at time intervals of 10 s. Inset shows the colour change of the solution.

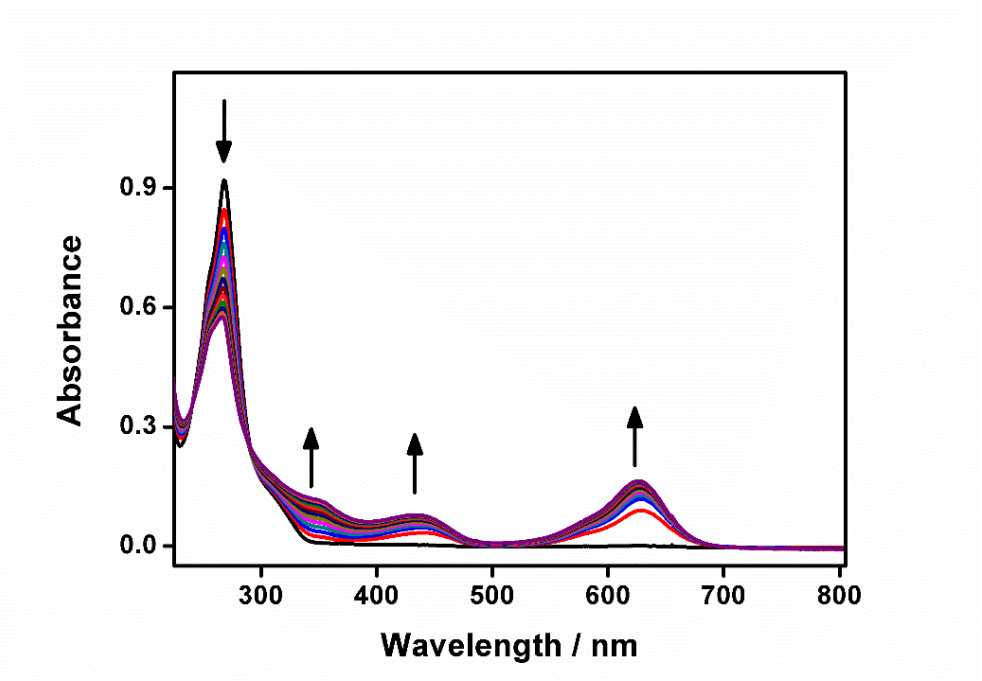

Fig. S5 UV–Visible absorption spectral traces of **L1** in MeCN solution at 298 K upon photo-irradiation at 254 nm ([**L1**] = 2.23×10^{-5} M). Spectra were taken at time intervals of 60 s.

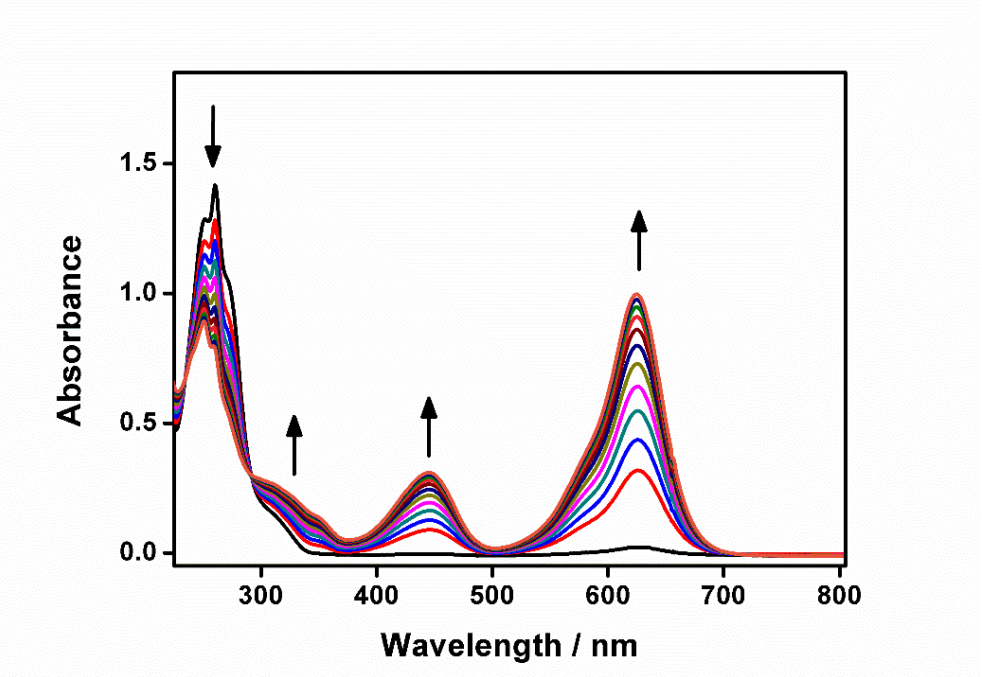

Fig. S6 UV–Visible absorption spectral traces of **L2** in MeCN solution at 298 K upon photo-irradiation at 254 nm ([**L2**] = 2.58 × 10^{-5} M). Spectra were taken at time intervals of 10 s.

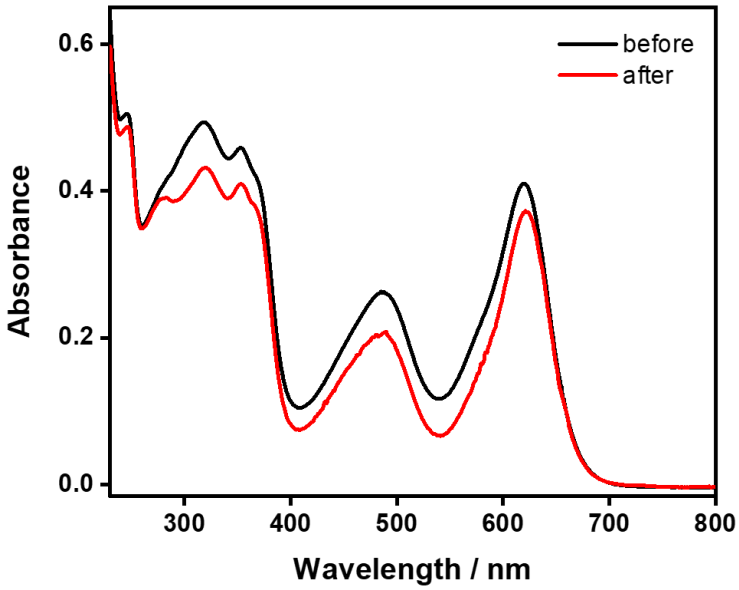

Fig. S7 Electronic absorption spectra of **1** in MeCN before and after standing the photo-irradiated solution for 48 hours in the dark at ambient conditions.

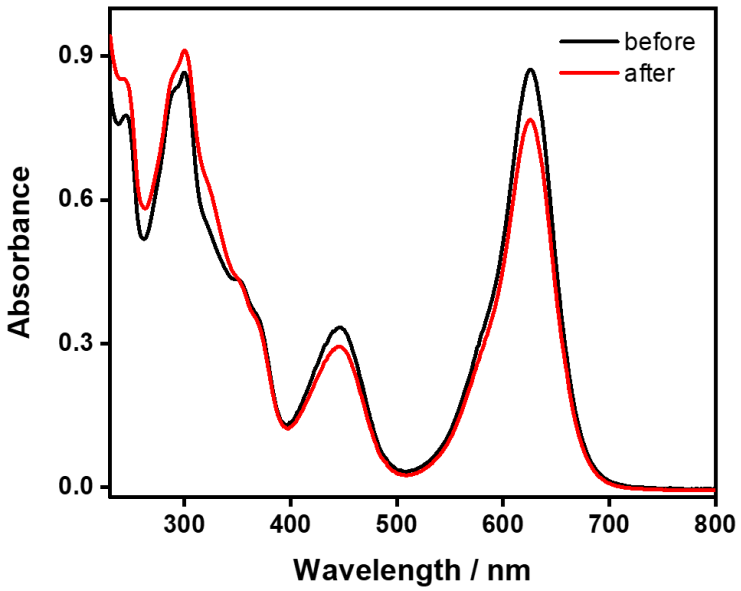

Fig. S8 Electronic absorption spectra of **2** in MeCN before and after standing the photo-irradiated solution for 48 hours in the dark at ambient conditions.

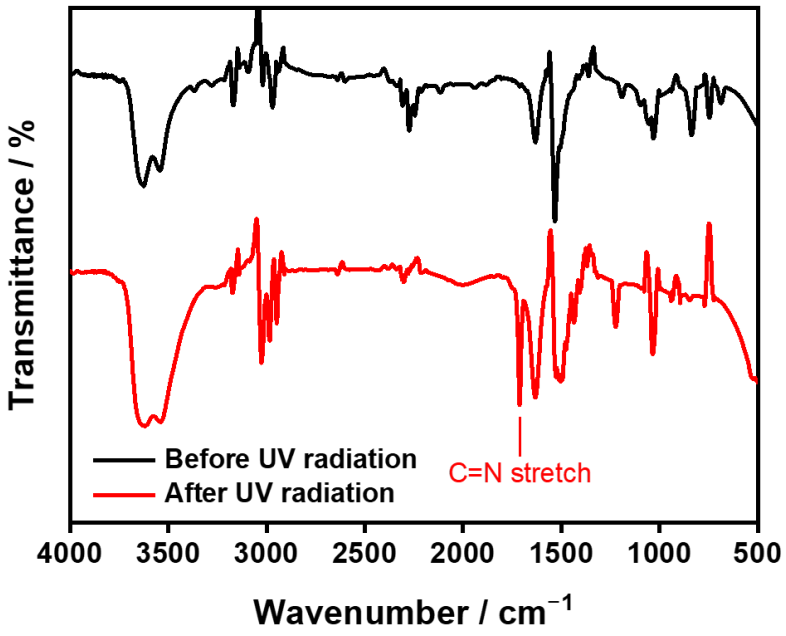

Fig. S9 FT-IR spectra of **2** before and after photo-irradiation at 254 nm for 2 min.

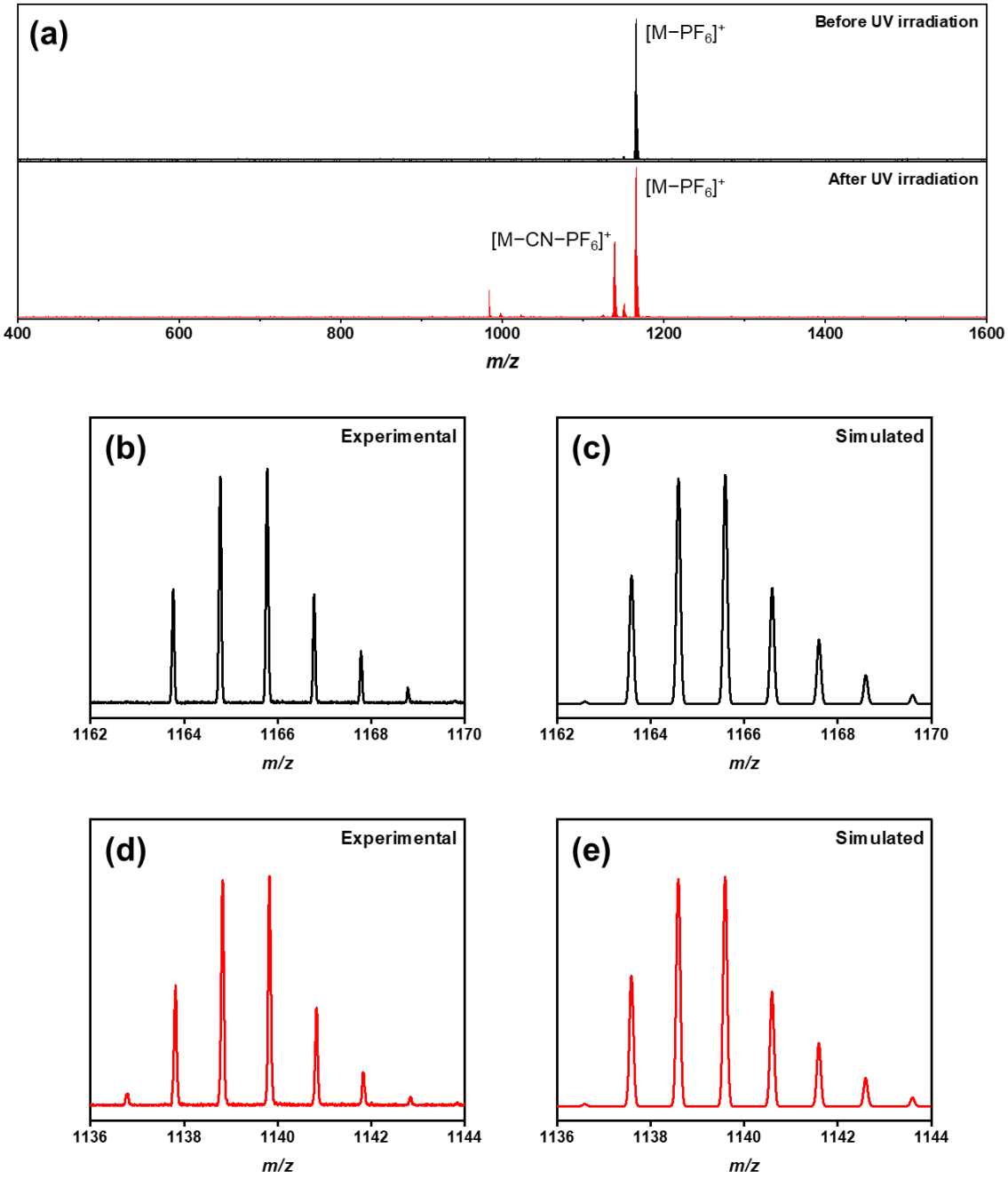

Fig. S10 (a) MALDI mass spectra of **1** before and after UV irradiation at 254 nm. (b) Expanded ion cluster of **1** corresponding to $[M-PF_6]^+$, and (c) its simulated isotopic pattern. (d) Expanded ion cluster of **1** corresponding to $[M-CN-PF_6]^+$, and (e) its simulated isotopic pattern.

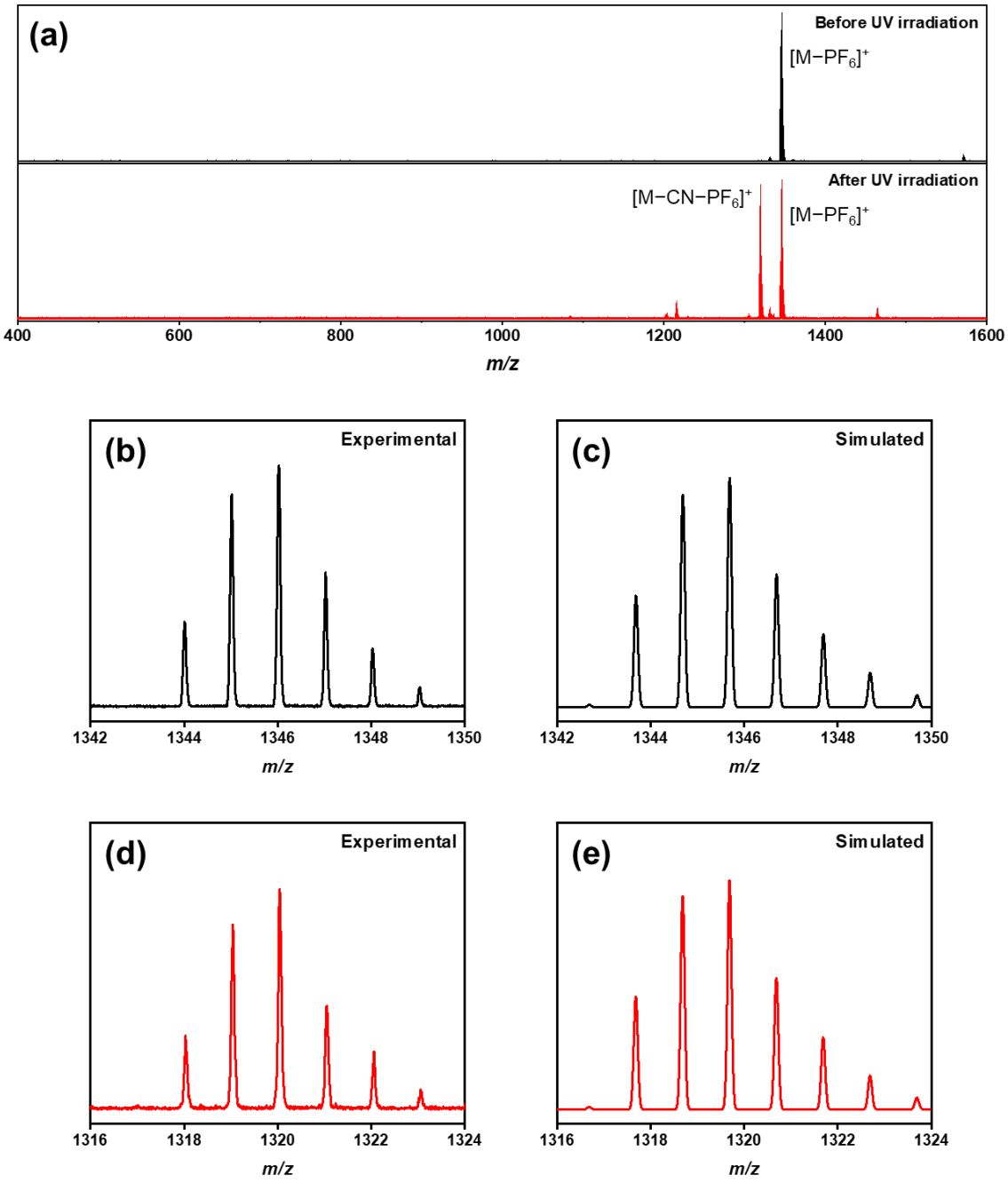

Fig. S11 (a) MALDI mass spectra of **2** before and after UV irradiation at 254 nm. (b) Expanded ion cluster of **2** corresponding to $[M-PF_6]^+$, and (c) its simulated isotopic pattern. (d) Expanded ion cluster of **2** corresponding to $[M-CN-PF_6]^+$, and (e) its simulated isotopic pattern.

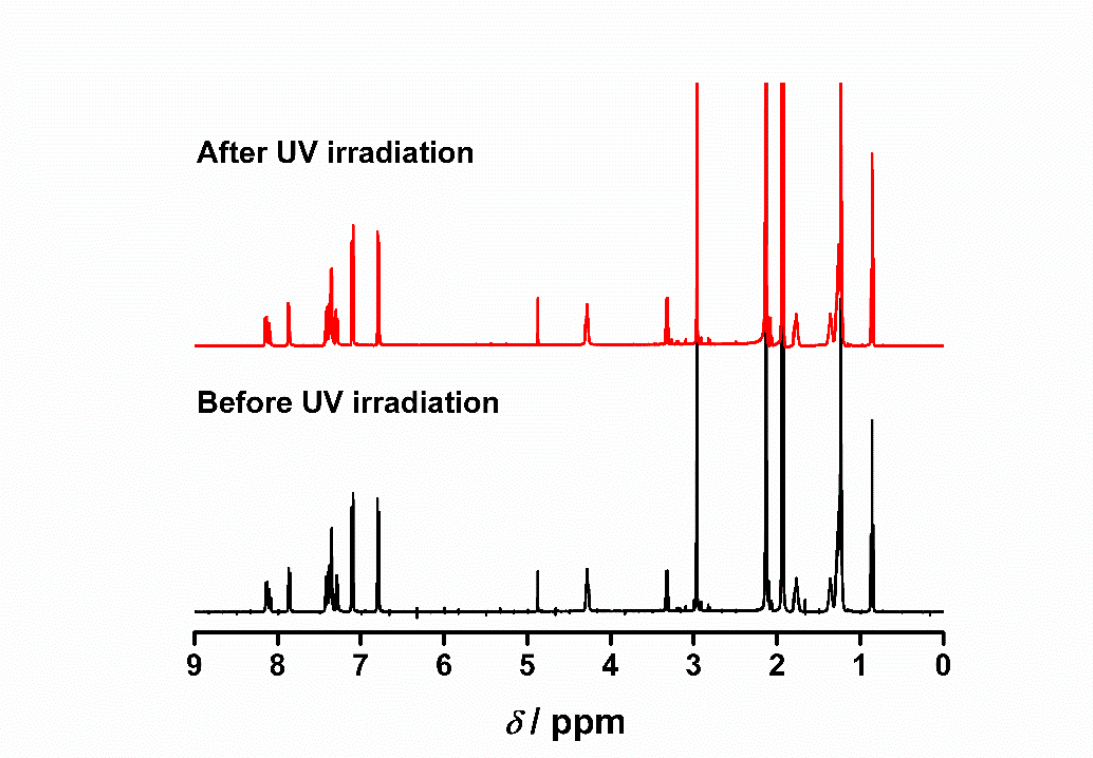

Fig. S12 ^{1}H NMR spectra of **1** before and after photo-irradiation at 254 nm in [D_3]-MeCN at 298 K ([**1**] = *ca*. 1 × 10^{-4} M).

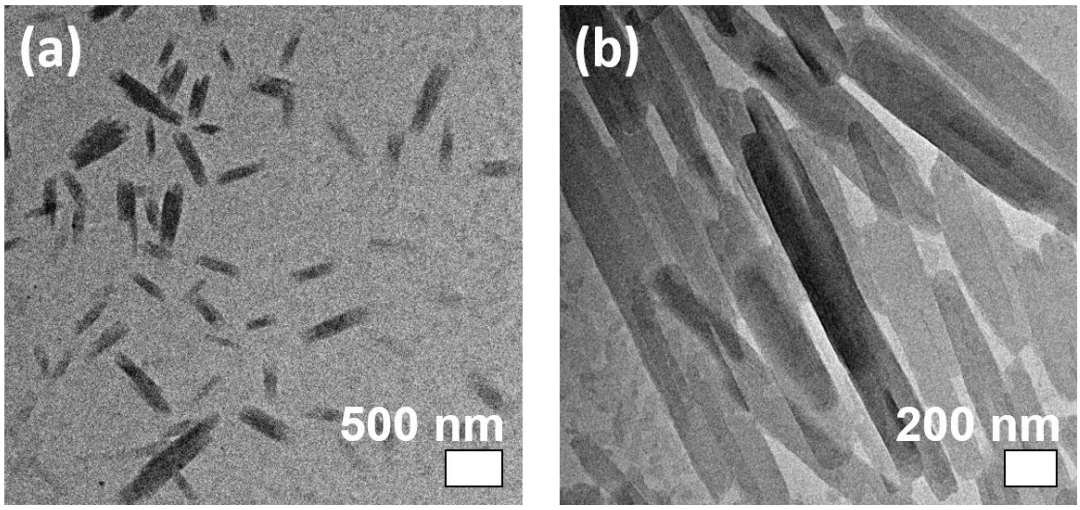

Fig. S13 TEM images of the aggregates prepared from a MeCN solution of **1** (a) before and (b) after UV irradiation ([**1**] = *ca*. 1×10^{-4} M).

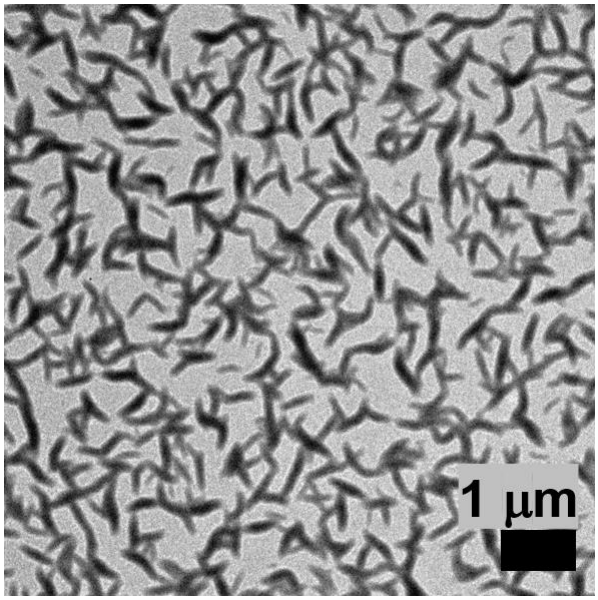

Fig. S14 TEM image of the aggregates prepared from a MeCN solution of **2** before UV irradiation ([**2**] = *ca*. 1×10^{-3} M).

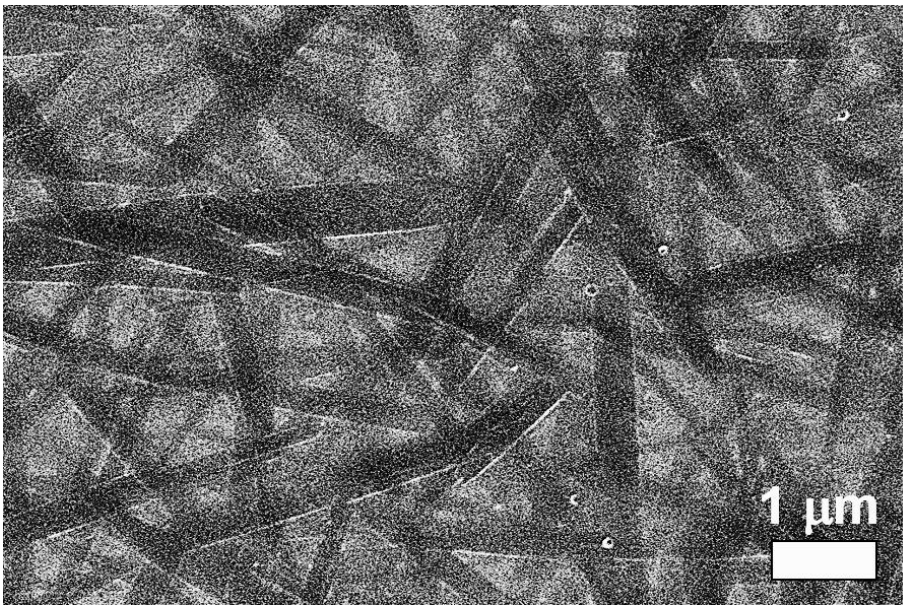

Fig. S15 SEM image of the aggregates prepared from a MeCN solution of **1** after UV irradiation ([**1**] = *ca*. 1 × 10^{-3} M).

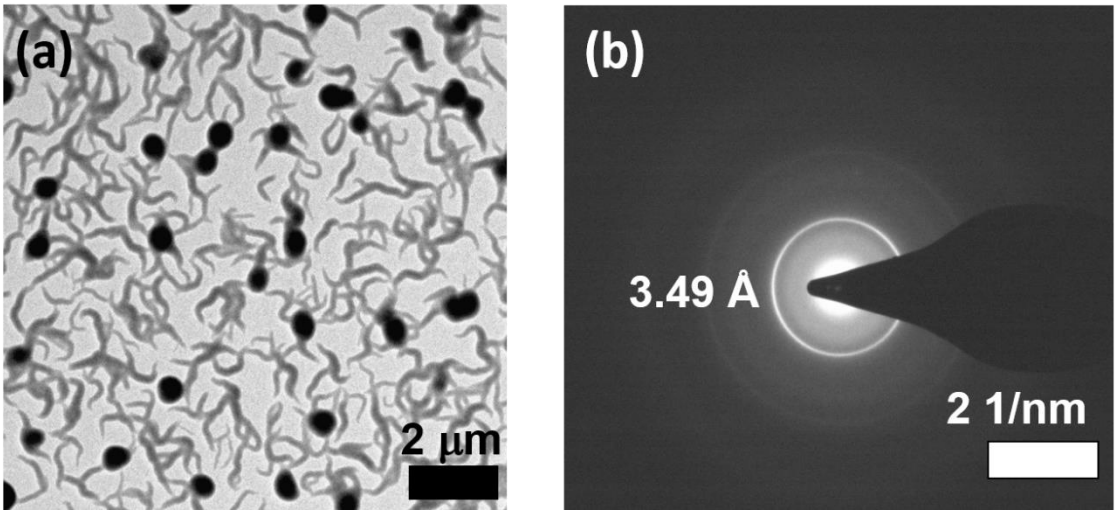

Fig. S16 Electron micrographs of the aggregates prepared from a MeCN solution of **2** after UV irradiation. (a) TEM image and (b) the corresponding SAED experiment of the worm-like aggregates ([**2**] = *ca*. 1 × 10^{-3} M).

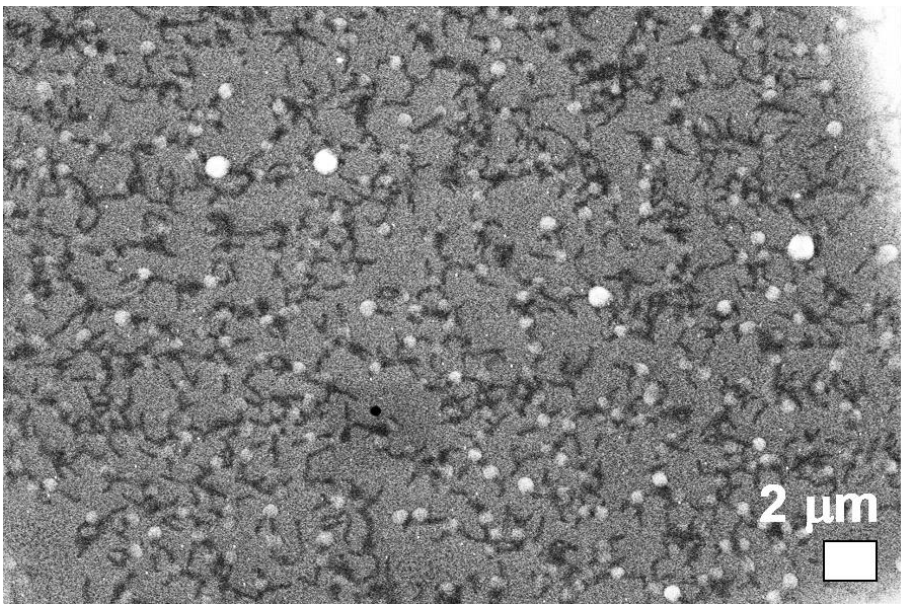

Fig. S17 SEM image of the aggregates prepared from a MeCN solution of **2** after UV irradiation ([**2**] = *ca*. 1 × 10^{-3} M).

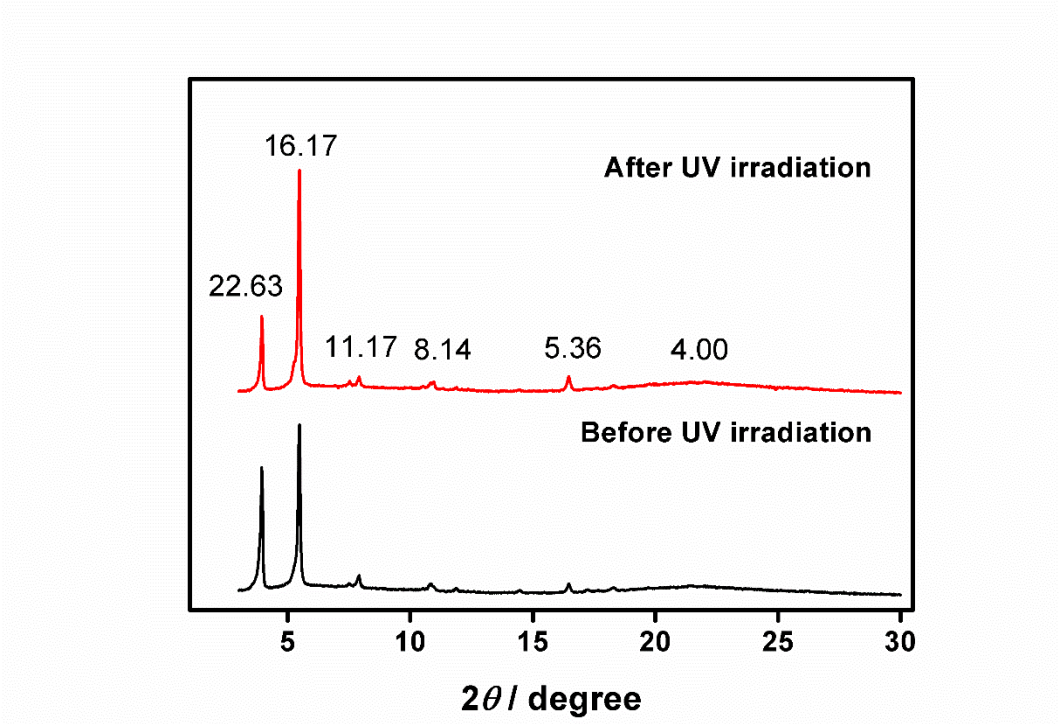

Fig. S18 XRD patterns of **1** in cast film prepared from MeCN solution before and after UV irradiation ([**1**] = *ca*. 1 × 10^{-3} M) with the *d* spacings (in Å).

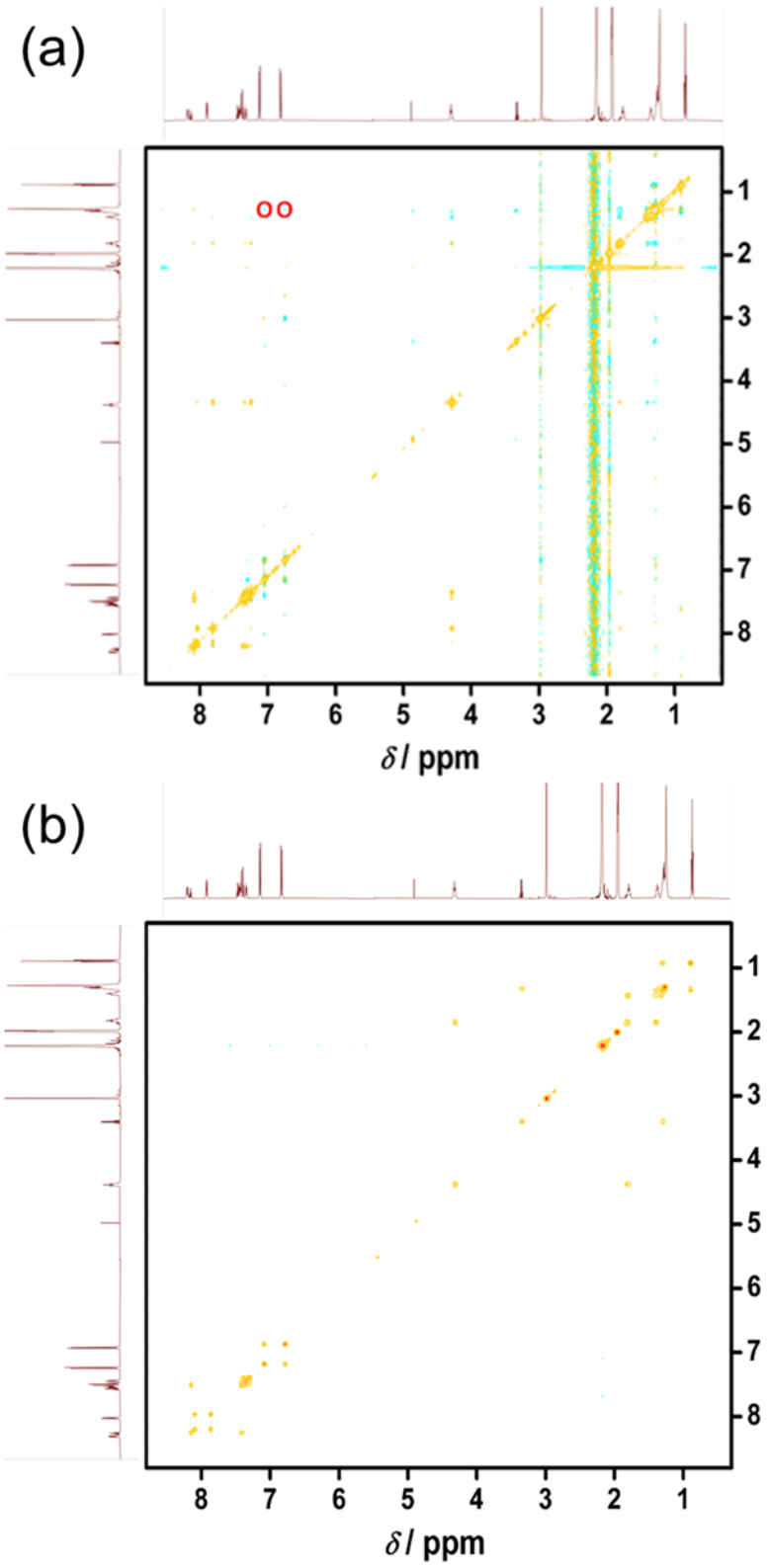

Fig. S19 (a) 2D NOESY and (b) 2D COSY NMR spectra of **1** in [D_3]-MeCN solution before UV irradiation at 298 K ([**1**] = *ca*. 1 × 10^{-3} M).

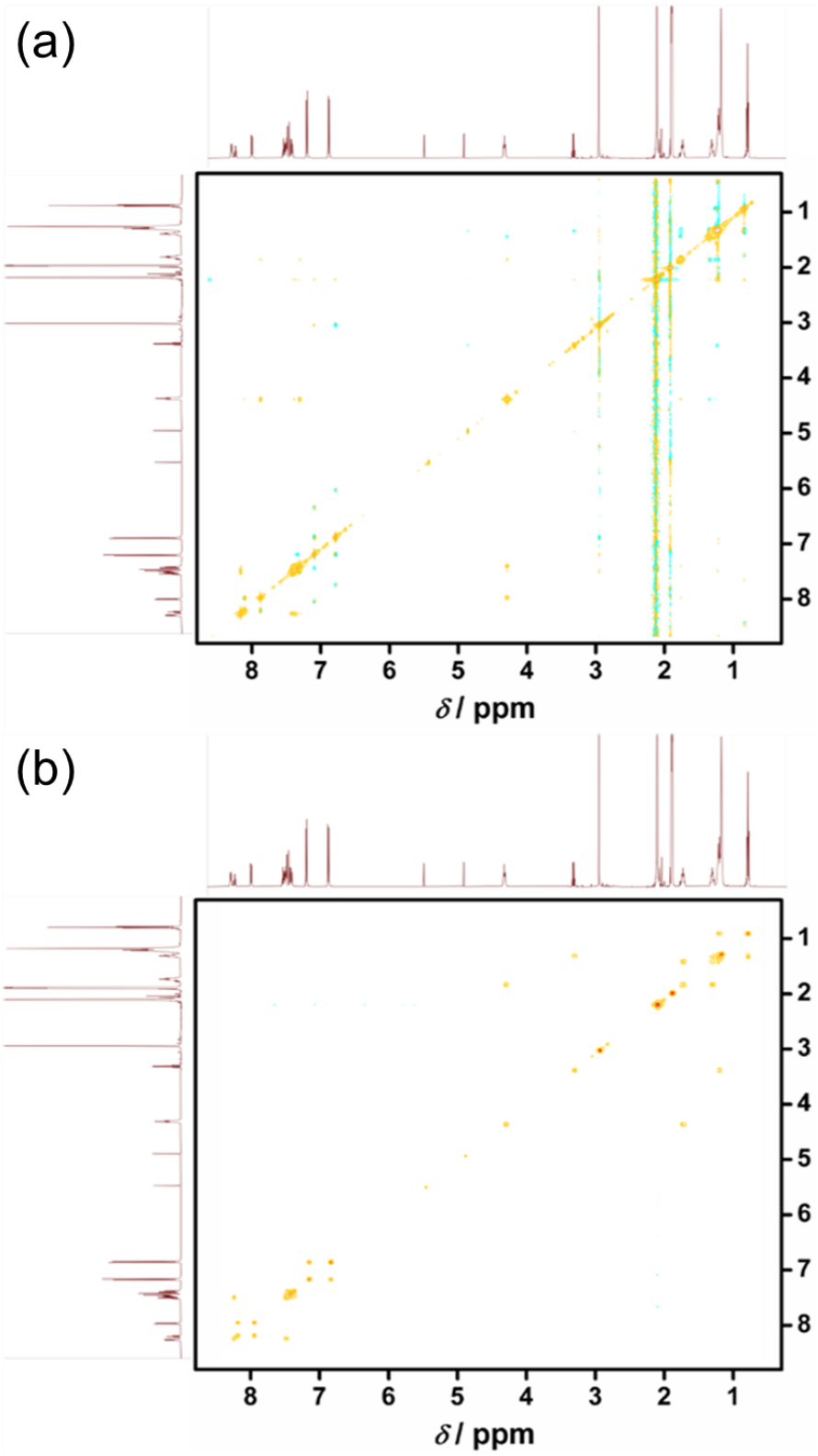

Fig. S20 (a) 2D NOESY and (b) 2D COSY NMR spectra of **1** in [D_3]-MeCN solution after UV irradiation at 298 K ([**1**] = *ca*. 1 × 10^{-3} M).

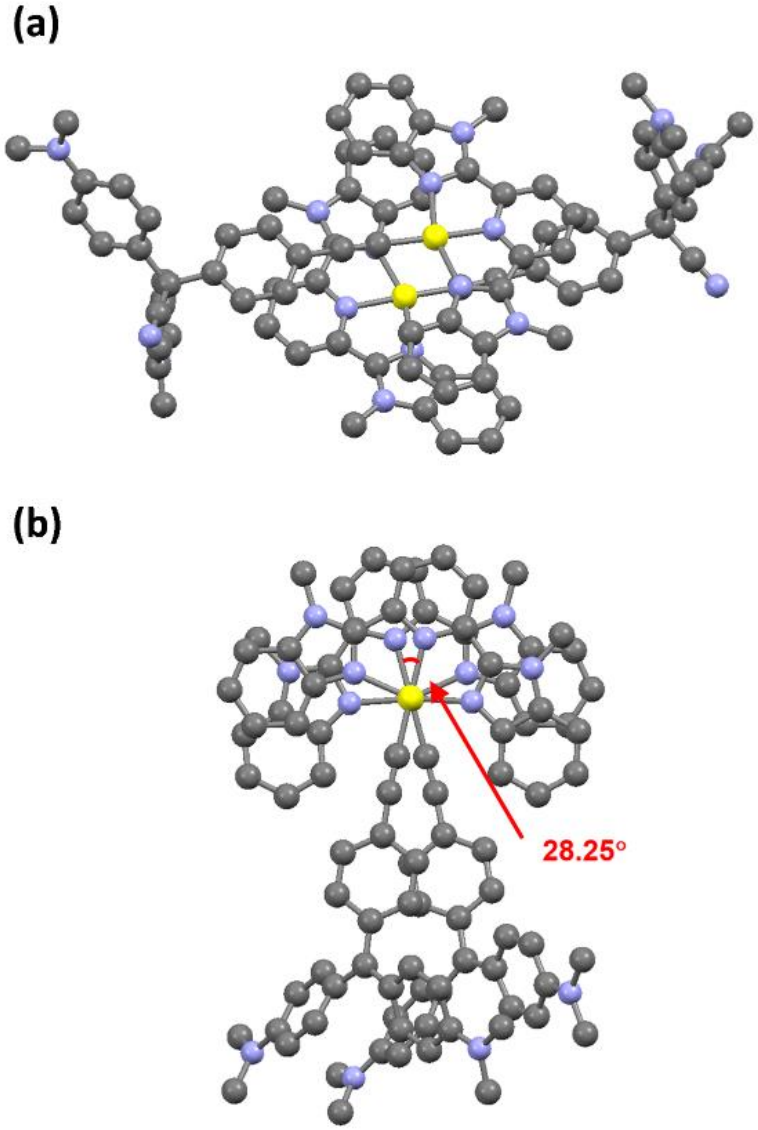

Fig. S21 Ground-state geometry of the dimer of (a) **1′** and (b) **1″** optimized at the M06 level. All hydrogen atoms were omitted for clarity.

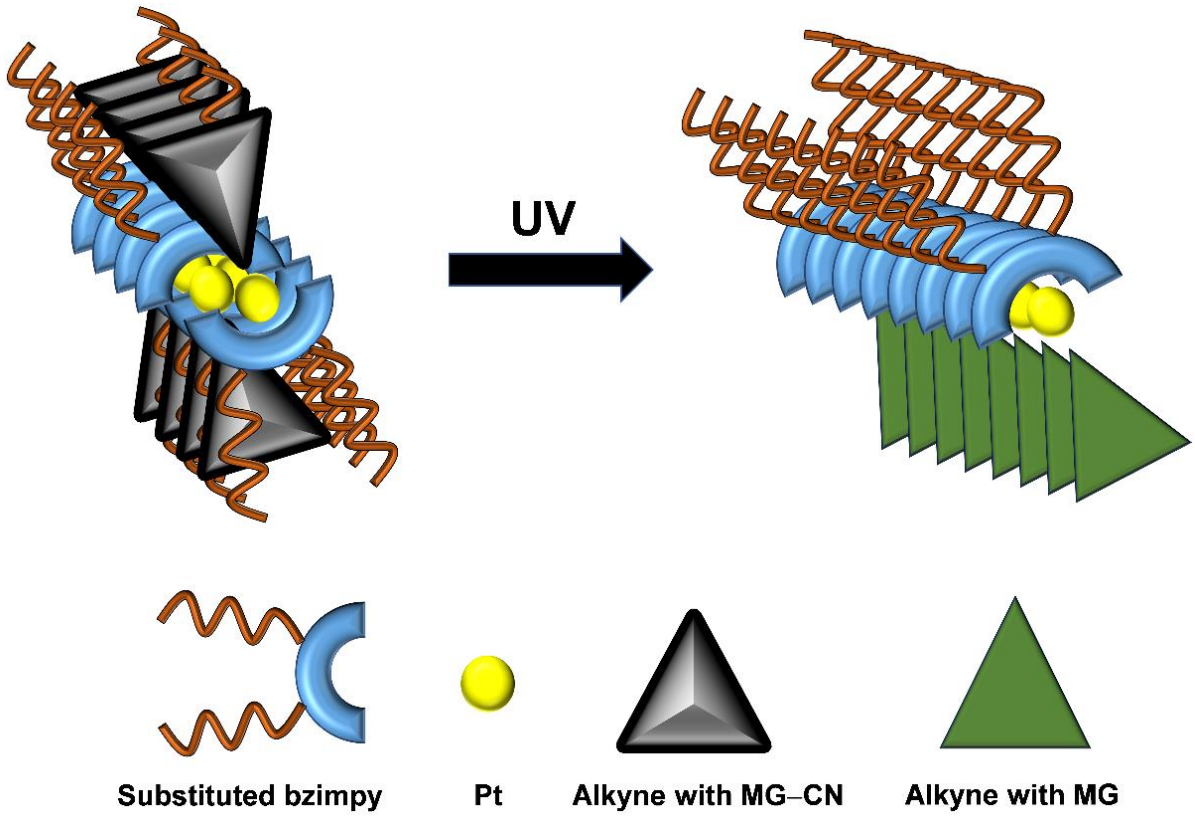

Fig. S22 A cartoon representation showing the proposed conformational changes of the malachite green-based alkynylplatinum(II) bzimpy complexes upon UV irradiation.

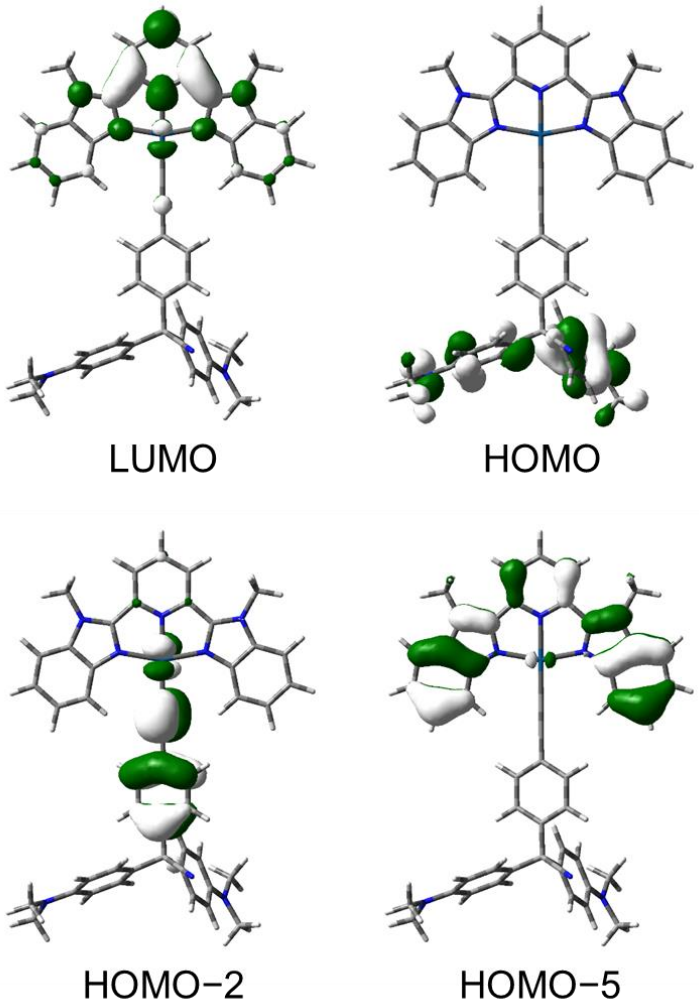

Fig. S23 Spatial plots (isovalue = 0.03) of selected frontier molecular orbitals of **1′** obtained from the PBE0/CPCM (toluene) calculation.

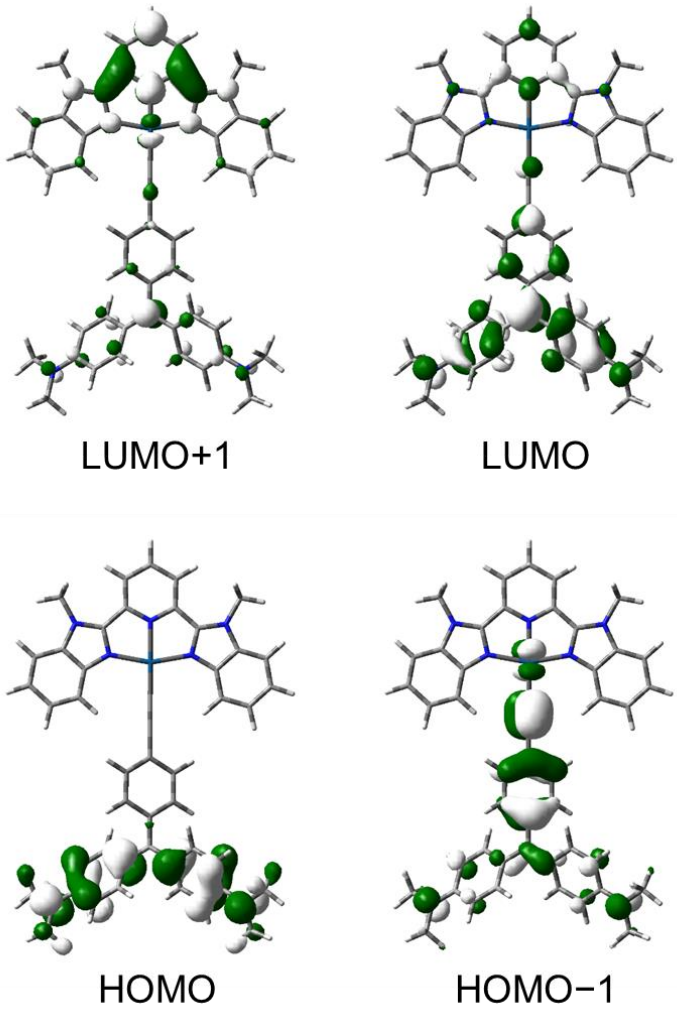

Fig. S24 Spatial plots (isovalue = 0.03) of selected frontier molecular orbitals of **1″** obtained from the PBE0/CPCM (toluene) calculation.

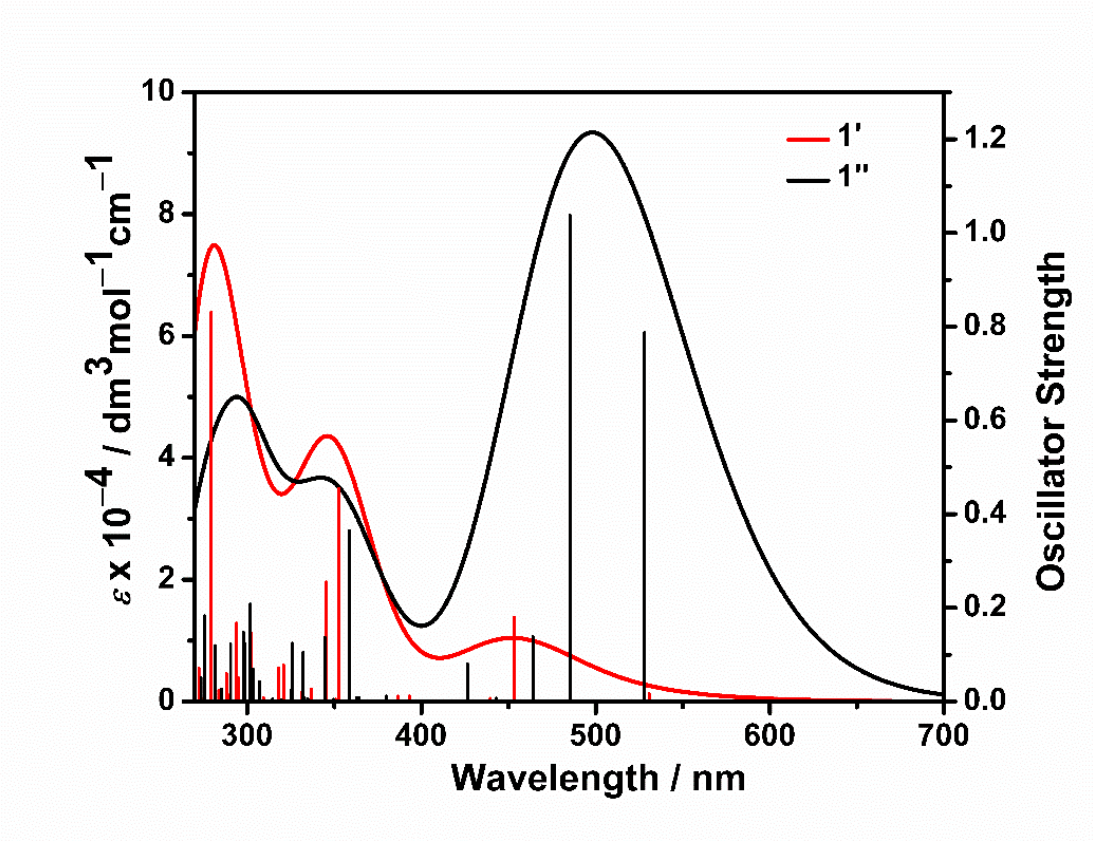

Fig. S25 Simulated electronic absorption spectra of **1′** and **1″** in toluene. The height of the vertical straight lines are calculated oscillator strengths of the corresponding vertical transitions.

Table S2 The first ten singlet (S_n) excited states of **1′** computed by TDDFT/CPCM (MeCN) at the optimized ground state geometries

S_n	Excitation[a] (Coefficient)[b]	Vertical excitation wavelength / nm	f [c]	Character[d]
S_1	H→L (0.70)	530	0.017	LLCT
S_2	H–1→L (0.71)	505	0.001	LLCT
S_3	H–2→L (0.69)	453	0.180	LLCT/MLCT
S_4	H→L+1 (0.70)	441	0.000	LLCT
S_5	H–3→L (0.69)	439	0.007	LLCT/MLCT
S_6	H–1→L+1 (0.71)	424	0.000	LLCT
S_7	H–4→L (0.70)	393	0.012	LLCT/MLCT
S_8	H–2→L+1 (0.70)	386	0.012	LLCT/MLCT
S_9	H–5→L (0.70)	352	0.455	ILCT/IL
S_{10}	H–11→L (0.70)	350	0.005	MLCT

[a] The orbitals involved in the excitation (H = HOMO and L = LUMO).

[b] The coefficients in the configuration interaction (CI) expansion that are less than 0.3 are not listed.

[c] Oscillator strengths.

[d] Character of the transition.

Table S3 The first ten singlet (S_n) excited states of **1″** computed by TDDFT/CPCM (MeCN) at the optimized ground state geometries

S_n	Excitation[a] (Coefficient)[b]	Vertical excitation wavelength / nm	f [c]	Character[d]
S_1	H→L (0.70)	528	0.788	IL/LLCT
S_2	H–1→L (0.69)	485	1.039	MLCT/LLCT
S_3	H→L+1 (0.70)	464	0.139	LLCT
S_4	H–2→L+1 (0.52)	443	0.008	IL/MLCT
	H–2→L (–0.47)			LLCT/MLCT
S_5	H–1→L+1 (0.67)	426	0.081	LLCT/MLCT
S_6	H→L+2 (0.71)	399	0.000	LLCT
S_7	H–4→L (0.58)	397	0.001	MLCT
S_8	H–2→L (0.48)	380	0.001	MLCT/LLCT
	H–2→L+1 (0.42)			IL/ILCT
S_9	H–1→L+2 (0.62)	380	0.012	LLCT/MLCT
S_{10}	H–3→L (0.52)	364	0.009	IL/MLCT
	H–4→L (0.43)			MLCT

[a] The orbitals involved in the excitation (H = HOMO and L = LUMO).

[b] The coefficients in the configuration interaction (CI) expansion that are less than 0.3 are not listed.

[c] Oscillator strengths.

[d] Character of the transition.

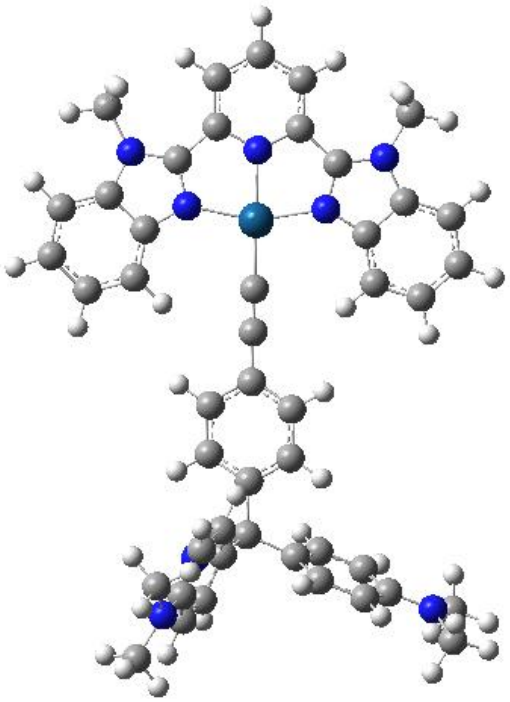

Table S4 Cartesian coordinates of the ground-state geometry of **1′** optimized at the PBE0 level.

1	C	-7.49985	1.478605	0.681355	50	C	2.909542	-1.31356	-1.47576
2	C	-8.2735	0.335554	0.494847	51	H	0.893003	-2.00787	-1.7228
3	C	-7.69459	-0.88799	0.167696	52	C	3.192355	0.702006	-0.19313
4	C	-6.31051	-0.94144	0.028874	53	H	1.396192	1.58184	0.589825
5	C	-6.12036	1.367178	0.531143	54	C	3.752584	-0.33646	-0.93771
6	H	-7.96808	2.419823	0.934842	55	H	3.329011	-2.13609	-2.0491
7	H	-9.35041	0.399894	0.607864	56	H	3.833195	1.464838	0.23689
8	H	-8.31057	-1.7656	0.027522	57	C	5.276505	-0.4551	-1.09911
9	C	-5.07187	2.377219	0.661055	58	C	5.84827	-1.50251	-0.13443
10	C	-3.01592	3.126592	0.61023	59	C	7.089441	-2.09535	-0.38352
11	C	-3.87048	4.199175	0.939778	60	C	5.196662	-1.83887	1.051857
12	C	-1.63407	3.308895	0.497773	61	C	7.659382	-2.99185	0.506439
13	C	-3.37751	5.484647	1.17323	62	H	7.629119	-1.85815	-1.29746
14	C	-1.14929	4.583777	0.729099	63	C	5.754884	-2.73013	1.958947
15	H	-0.98851	2.477569	0.237885	64	H	4.229463	-1.40305	1.28272
16	C	-2.00704	5.652777	1.062567	65	C	7.011314	-3.32662	1.717528
17	H	-4.02941	6.313471	1.426698	66	H	8.615949	-3.43537	0.255853
18	H	-0.08226	4.769038	0.651815	67	C	5.968235	0.906486	-0.94341

19	H	-1.58136	6.636404	1.235227	68	C	5.811216	1.892046	-1.92271
20	C	-5.43844	-2.06753	-0.30074	69	C	6.717974	1.228931	0.186223
21	C	-3.51915	-3.05194	-0.67416	70	C	6.379895	3.148201	-1.78826
22	C	-4.54348	-4.01193	-0.80879	71	H	5.234264	1.676158	-2.81931
23	C	-2.17538	-3.39673	-0.84951	72	C	7.29184	2.484847	0.340866
24	C	-4.26505	-5.3426	-1.12712	73	H	6.86567	0.488541	0.966215
25	C	-1.90294	-4.71602	-1.16465	74	C	7.12983	3.488073	-0.63847
26	H	-1.39621	-2.65106	-0.73777	75	H	6.240749	3.868415	-2.58588
27	C	-2.93102	-5.67204	-1.30205	76	H	7.873082	2.680111	1.234419
28	H	-5.04861	-6.08526	-1.2307	77	C	5.54268	-0.92206	-2.4731
29	H	-0.87239	-5.02581	-1.30931	78	N	5.760812	-1.2846	-3.55362
30	H	-2.66943	-6.69608	-1.55015	79	N	7.671983	4.741228	-0.48051
31	N	-5.73568	-3.35609	-0.56813	80	C	7.684115	5.652162	-1.60437
32	N	-4.11066	-1.85353	-0.36025	81	H	8.111702	6.603321	-1.28489
33	N	-3.79512	2.008352	0.446147	82	H	8.274841	5.274816	-2.45276
34	N	-5.15509	3.689829	0.960252	83	H	6.667672	5.851755	-1.95961
35	C	-7.05522	-3.96148	-0.61498	84	C	8.632346	4.962133	0.578608
36	H	-7.53622	-3.8954	0.362816	85	H	8.947591	6.006263	0.56044
37	H	-7.66605	-3.46844	-1.37358	86	H	8.188338	4.769254	1.561224
38	H	-6.94203	-5.0103	-0.88186	87	H	9.527196	4.329602	0.478099
39	C	-6.36051	4.443521	1.257756	88	H	5.201692	-2.96367	2.861057
40	H	-7.02985	4.437782	0.39494	89	N	7.581289	-4.19083	2.618732
41	H	-6.86121	4.02001	2.130512	90	C	6.798974	-4.66344	3.739162
42	H	-6.07933	5.471309	1.478357	91	H	7.419957	-5.31283	4.357602
43	N	-5.58147	0.174948	0.213698	92	H	6.464774	-3.83027	4.367351
44	Pt	-3.59711	0.056122	0.003892	93	H	5.910295	-5.23191	3.426178
45	C	-1.66159	-0.05743	-0.21063	94	C	8.758823	-4.9386	2.237355
46	C	-0.44515	-0.12488	-0.35973	95	H	8.580779	-5.59697	1.374018
47	C	0.965745	-0.2013	-0.54397	96	H	9.590393	-4.26969	1.988485
48	C	1.5371	-1.24835	-1.28943	97	H	9.074944	-5.55638	3.078694
49	C	1.818842	0.769621	0.005676					

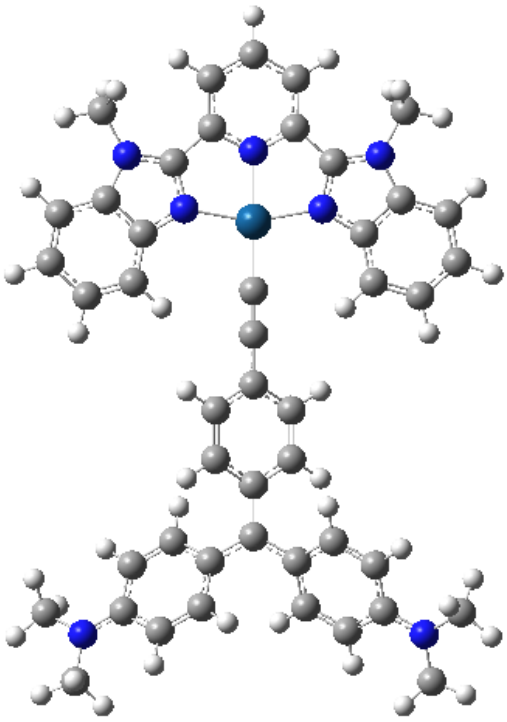

Table S5 Cartesian coordinates of the ground-state geometry of **1″** optimized at the PBE0 level.

1	C	7.543881	1.196489	0.209122	49	C	-1.79901	1.065015	0.578736
2	C	8.224492	-6.3E-05	-0.00044	50	C	-3.18211	-1.06774	-0.56818
3	C	7.543803	-1.19661	-0.20982	51	H	-1.25549	-1.88319	-1.04061
4	C	6.15213	-1.16883	-0.19879	52	C	-3.1821	1.067894	0.568763
5	C	6.152201	1.168733	0.1985	53	H	-1.25546	1.88326	1.04126
6	H	8.092033	2.113655	0.374221	54	C	-3.90254	0.000094	0.000277
7	H	9.309312	-7.2E-05	-0.0006	55	H	-3.72123	-1.88585	-1.03554
8	H	8.091886	-2.11378	-0.37511	56	H	-3.72117	1.886061	1.03607
9	C	5.184296	2.249866	0.379088	57	C	-5.36456	0.00008	0.000128
10	C	3.181053	3.120875	0.527907	58	C	-6.06146	-1.22186	0.240832
11	C	4.127199	4.151881	0.703739	59	C	-7.34917	-1.4693	-0.30747
12	C	1.808124	3.38312	0.569835	60	C	-5.49376	-2.25691	1.032206
13	C	3.738359	5.474047	0.928896	61	C	-8.02021	-2.64376	-0.08481
14	C	1.42649	4.694079	0.792707	62	H	-7.78861	-0.73424	-0.97428
15	H	1.089042	2.583802	0.43123	63	C	-6.16451	-3.42412	1.289845
16	C	2.376244	5.721671	0.969813	64	H	-4.52401	-2.09881	1.493373
17	H	4.460767	6.271449	1.064597	65	C	-7.45702	-3.66145	0.738202
18	H	0.369742	4.940425	0.832265	66	H	-8.97852	-2.80143	-0.56468

19	H	2.030618	6.73627	1.142292	67	H	-5.70556	-4.16387	1.934326
20	C	5.184165	-2.24994	-0.3792	68	C	-6.06153	1.221969	-0.24071
21	C	3.180874	-3.12087	-0.5278	69	C	-5.4938	2.257036	-1.03203
22	C	4.126959	-4.15188	-0.70391	70	C	-7.34934	1.469334	0.3074
23	C	1.807929	-3.38306	-0.56959	71	C	-6.16461	3.424187	-1.28981
24	C	3.738044	-5.474	-0.92923	72	H	-4.52395	2.099026	-1.493
25	C	1.426222	-4.69397	-0.7926	73	C	-8.02046	2.643712	0.08455
26	H	1.088892	-2.58374	-0.43078	74	H	-7.7888	0.734286	0.974212
27	C	2.375916	-5.72157	-0.97	75	C	-7.45727	3.661373	-0.73849
28	H	4.460412	-6.2714	-1.06516	76	H	-5.70558	4.164005	-1.93416
29	H	0.36946	-4.94028	-0.83204	77	H	-8.97882	2.801355	0.564333
30	H	2.03023	-6.73613	-1.14258	78	N	-8.11677	-4.80978	0.978356
31	N	5.37486	-3.56671	-0.60325	79	N	-8.1171	4.809612	-0.97895
32	N	3.872412	-1.95143	-0.32928	80	C	-7.50738	-5.85309	1.783226
33	N	3.872524	1.951389	0.329468	81	H	-7.3201	-5.50839	2.806611
34	N	5.375068	3.566644	0.603033	82	H	-8.18254	-6.70618	1.827106
35	C	6.645473	-4.26328	-0.71407	83	H	-6.55876	-6.18609	1.347981
36	H	7.207856	-3.88222	-1.56865	84	C	-9.4439	-5.02427	0.430427
37	H	7.220845	-4.14107	0.205731	85	H	-9.42505	-5.0411	-0.6656
38	H	6.446274	-5.32192	-0.86638	86	H	-9.82158	-5.98326	0.78182
39	C	6.645723	4.26316	0.713666	87	H	-10.1372	-4.24087	0.755173
40	H	7.208319	3.881898	1.568024	88	C	-9.44419	5.024252	-0.43098
41	H	7.220848	4.141166	-0.20631	89	H	-9.82217	5.982865	-0.78308
42	H	6.44659	5.321761	0.866334	90	H	-10.1373	4.240438	-0.75506
43	N	5.514092	-4.7E-05	-4.8E-05	91	H	-9.42524	5.041887	0.665038
44	Pt	3.514603	-1.9E-05	0.000134	92	C	-7.50728	5.853099	-1.78327
45	C	1.566659	0.000004	0.000294	93	H	-8.1829	6.705763	-1.82829
46	C	0.338763	0.000003	0.000352	94	H	-6.55939	6.186762	-1.34689
47	C	-1.08142	0.000031	0.000332	95	H	-7.31847	5.508245	-2.80632
48	C	-1.79903	-1.06493	-0.57809					

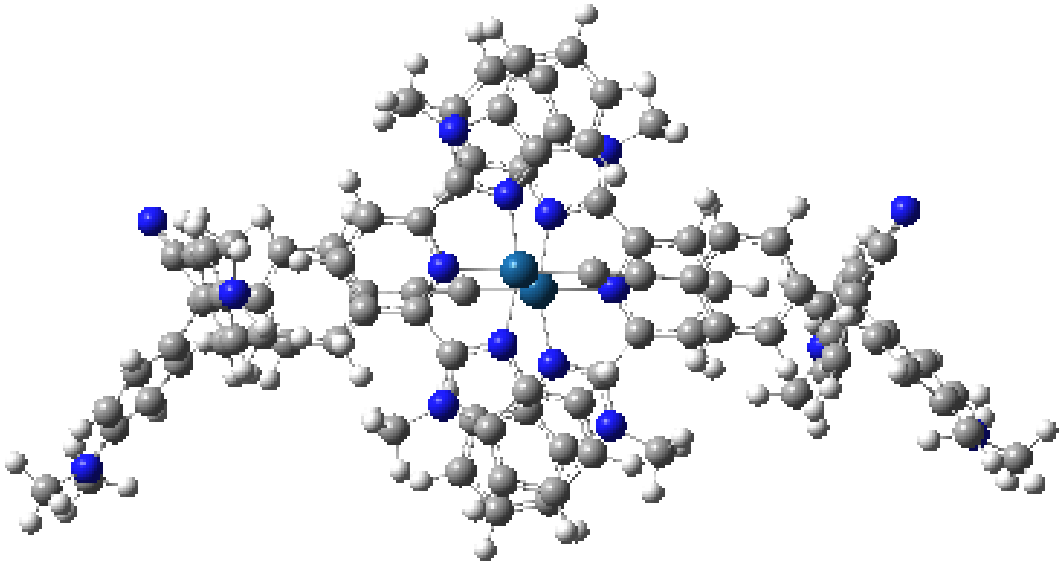

Table S6 Cartesian coordinates of the ground-state geometry of dimer of **1′** optimized at the PBE0 level.

1	C	4.241716	1.612316	-2.02352	98	C	7.10069	0.353357	1.015293
2	C	4.944502	0.412272	-1.95403	99	H	7.061847	2.491496	0.736087
3	C	4.286218	-0.80329	-1.79203	100	H	6.795456	-1.74746	1.398579
4	C	2.895766	-0.79201	-1.70888	101	C	8.55088	0.165354	0.539866
5	C	2.853792	1.566989	-1.93303	102	C	8.464311	-0.19578	-0.9505
6	H	4.768621	2.548021	-2.15218	103	C	8.62611	0.754268	-1.95797
7	H	6.02603	0.425868	-2.02595	104	C	8.06121	-1.47978	-1.33085
8	H	4.851972	-1.72342	-1.744	105	C	8.390173	0.447883	-3.29348
9	C	1.868278	2.643247	-2.01824	106	H	8.925464	1.768794	-1.70815
10	C	-0.1505	3.487522	-2.1013	107	C	7.820595	-1.80298	-2.65657
11	C	0.776521	4.543146	-2.22774	108	H	7.923477	-2.25001	-0.57793
12	C	-1.52797	3.725511	-2.12638	109	C	7.978145	-0.8439	-3.6838
13	C	0.363015	5.866198	-2.39006	110	H	8.518934	1.229977	-4.03219
14	C	-1.93459	5.039425	-2.28551	111	C	9.34305	-0.84704	1.37727
15	H	-2.22976	2.904612	-2.03235	112	C	9.142407	-0.94448	2.757075
16	C	-1.00401	6.091003	-2.41605	113	C	10.37626	-1.60177	0.818313
17	H	1.071155	6.681816	-2.48603	114	C	9.908076	-1.78969	3.544984
18	H	-2.99569	5.268017	-2.3141	115	H	8.371962	-0.34524	3.23456
19	H	-1.36851	7.106177	-2.53875	116	C	11.15337	-2.45278	1.590317
20	C	1.946451	-1.89856	-1.59115	117	H	10.58636	-1.52594	-0.24451
21	C	-0.04404	-2.81056	-1.5522	118	C	10.9298	-2.58619	2.979169
22	C	0.915794	-3.84324	-1.51853	119	H	9.710441	-1.8251	4.609866

23	C	-1.41348	-3.09234	-1.54455	120	H	11.94239	-3.01545	1.105313
24	C	0.542203	-5.18819	-1.48821	121	C	9.284531	1.43189	0.695148
25	C	-1.78012	-4.42642	-1.51207	122	N	9.887276	2.41357	0.835758
26	H	-2.13774	-2.2867	-1.5696	123	N	11.66989	-3.4512	3.743954
27	C	-0.81701	-5.45656	-1.48755	124	C	11.54902	-3.40897	5.184725
28	H	1.274172	-5.98812	-1.46571	125	H	12.18958	-4.17886	5.616589
29	H	-2.83377	-4.6891	-1.50695	126	H	11.84652	-2.43731	5.606017
30	H	-1.1494	-6.48975	-1.46452	127	H	10.52111	-3.61729	5.502014
31	N	2.155389	-3.23198	-1.53453	128	C	12.83719	-4.08424	3.170718
32	N	0.630108	-1.6161	-1.59418	129	H	13.2787	-4.75146	3.911869
33	N	0.561951	2.321794	-1.97071	130	H	12.56979	-4.68987	2.297661
34	N	2.035018	3.97485	-2.16291	131	H	13.60278	-3.35805	2.859871
35	C	3.435755	-3.91699	-1.48752	132	H	7.504091	-2.81224	-2.89187
36	H	3.976441	-3.77443	-2.42612	133	N	7.738279	-1.15973	-5.00054
37	H	4.028646	-3.54248	-0.65132	134	C	7.034061	-2.38702	-5.30571
38	H	3.253835	-4.9794	-1.33783	135	H	6.9351	-2.47853	-6.38803
39	C	3.291648	4.701319	-2.20426	136	H	7.590296	-3.26079	-4.95157
40	H	3.888651	4.461839	-1.32288	137	H	6.026489	-2.41916	-4.8622
41	H	3.842861	4.455152	-3.11443	138	C	7.656651	-0.08853	-5.97023
42	H	3.073042	5.767295	-2.19807	139	H	6.835312	0.613577	-5.75874
43	N	2.237308	0.379851	-1.77974	140	H	8.591354	0.480152	-6.0069
44	Pt	0.239004	0.350303	-1.7485	141	H	7.495998	-0.51832	-6.95989
45	C	-4.31082	-0.19417	1.890482	142	C	-1.70951	0.311333	-1.77493
46	C	-4.94446	1.044838	1.853588	143	C	-2.93595	0.278185	-1.74586
47	C	-4.22159	2.223	1.679677	144	C	-4.34895	0.222579	-1.58488
48	C	-2.8378	2.133633	1.556071	145	C	-5.12054	1.394336	-1.54042
49	C	-2.92463	-0.2252	1.762322	146	C	-4.99598	-1.00949	-1.38229
50	H	-4.8897	-1.09654	2.031949	147	C	-6.47584	1.337478	-1.24278
51	H	-6.02215	1.093653	1.962384	148	H	-4.64217	2.354961	-1.70781
52	H	-4.73331	3.175392	1.656361	149	C	-6.35148	-1.06014	-1.09523
53	C	-2.00104	-1.35714	1.802224	150	H	-4.42178	-1.92955	-1.43718
54	C	-0.03266	-2.31414	1.848793	151	C	-7.10334	0.114491	-0.99688
55	C	-1.01628	-3.32268	1.915211	152	H	-7.04227	2.262693	-1.18061
56	C	1.329899	-2.6258	1.859729	153	H	-6.8251	-2.02316	-0.93378
57	C	-0.67432	-4.67309	2.003543	154	C	-8.54767	0.054831	-0.47147
58	C	1.665422	-3.9659	1.946902	155	C	-8.44502	0.10348	1.059824
59	H	2.071873	-1.83774	1.804872	156	C	-9.33604	-1.15002	-1.00222
60	C	0.67892	-4.97116	2.02026	157	C	-9.28674	1.232519	-0.95453

61	H	-1.42483	-5.45431	2.053044	158	C	-8.69727	1.260877	1.79457
62	H	2.712446	-4.25351	1.960193	159	C	-7.95154	-1.00737	1.752304
63	H	0.987843	-6.00979	2.086098	160	C	-9.20197	-1.54794	-2.33614
64	C	-1.82966	3.182272	1.403602	161	C	-10.2882	-1.80819	-0.22277
65	C	0.207347	3.979481	1.288497	162	N	-9.88861	2.14071	-1.35402
66	C	-0.69649	5.056618	1.179018	163	C	-8.46582	1.319431	3.164536
67	C	1.589807	4.186425	1.25348	164	H	-9.07102	2.152492	1.297978
68	C	-0.2543	6.373289	1.041545	165	C	-7.71741	-0.96896	3.117013
69	C	2.024608	5.493232	1.112705	166	H	-7.73447	-1.92695	1.21698
70	H	2.274353	3.350293	1.341413	167	C	-9.95108	-2.58736	-2.86319
71	C	1.117101	6.567868	1.009846	168	H	-8.49559	-1.03498	-2.98354
72	H	-0.94457	7.205629	0.959842	169	C	-11.0474	-2.85219	-0.73244
73	H	3.090334	5.699088	1.084644	170	H	-10.4473	-1.50358	0.807217
74	H	1.503629	7.576692	0.903414	171	C	-7.9701	0.202103	3.86912
75	N	-1.96692	4.515818	1.244064	172	H	-8.67041	2.248541	3.683099
76	N	-0.53016	2.829895	1.422104	173	H	-7.32861	-1.85796	3.599539
77	N	-0.67925	-1.10617	1.775708	174	C	-10.8864	-3.28774	-2.06653
78	N	-2.24177	-2.68366	1.870687	175	H	-9.80681	-2.85608	-3.90302
79	C	-3.20636	5.259516	1.107821	176	H	-11.7738	-3.32841	-0.08431
80	H	-3.82625	4.807218	0.332224	177	N	-7.74142	0.245464	5.222735
81	H	-3.74404	5.283823	2.058127	178	N	-11.6014	-4.3447	-2.56829
82	H	-2.96616	6.277849	0.808293	179	C	-6.99613	-0.82809	5.843359
83	C	-3.53833	-3.33789	1.845123	180	C	-7.77533	1.523531	5.89975
84	H	-4.08874	-3.13206	2.765743	181	C	-11.5626	-4.61934	-3.98786
85	H	-4.10826	-2.9966	0.978756	182	C	-12.6753	-4.91442	-1.78531
86	H	-3.37957	-4.41118	1.759056	183	H	-6.92529	-0.63714	6.914834
87	N	-2.24505	0.92575	1.609405	184	H	-7.50544	-1.78874	5.713071
88	Pt	-0.24724	0.847629	1.588261	185	H	-5.97595	-0.92369	5.440207
89	C	1.699882	0.772742	1.652543	186	H	-7.01834	2.225938	5.518473
90	C	2.925727	0.711719	1.651865	187	H	-8.75817	1.996193	5.799961
91	C	4.339954	0.607624	1.526722	188	H	-7.59264	1.366124	6.963481
92	C	5.125497	1.735651	1.242708	189	H	-12.1687	-5.50181	-4.19548
93	C	4.974816	-0.64531	1.599051	190	H	-11.951	-3.78523	-4.5907
94	C	6.484438	1.605457	0.985292	191	H	-10.5412	-4.83345	-4.32167
95	H	4.65648	2.714141	1.195626	192	H	-13.0909	-5.76857	-2.32123
96	C	6.332535	-0.76728	1.348444	193	H	-12.3088	-5.2773	-0.81866
97	H	4.387938	-1.52792	1.835597	194	H	-13.4884	-4.19831	-1.59472

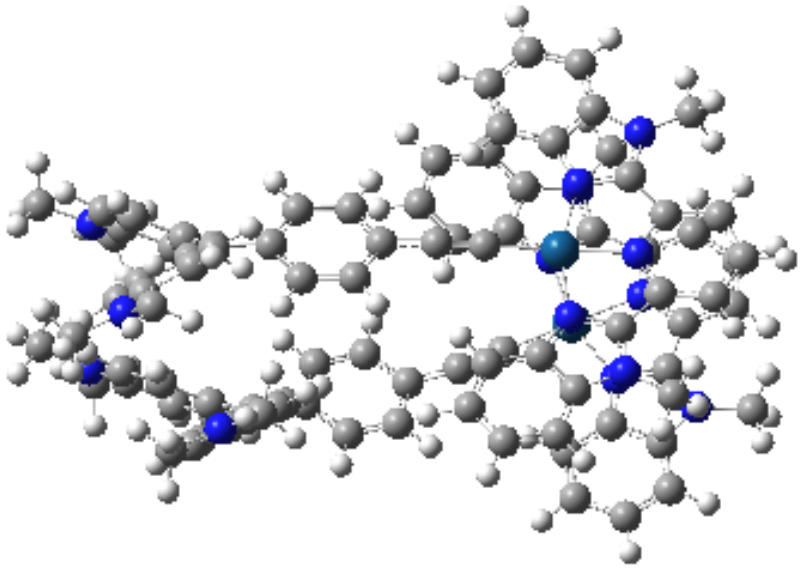

Table S7 Cartesian coordinates of the ground-state geometry of dimer of **1″** optimized at the PBE0 level.

1	C	7.25859	2.553333	-0.72254	96	C	7.368099	-0.18634	2.027896
2	C	8.236051	1.596853	-0.98867	97	C	7.764842	-1.46218	1.633517
3	C	7.900167	0.313586	-1.41377	98	C	6.83629	-2.42113	1.235821
4	C	6.550433	0.005184	-1.56117	99	C	5.489311	-2.06635	1.228917
5	C	5.923839	2.191274	-0.88491	100	C	6.008965	0.114326	2.000056
6	H	7.539533	3.549407	-0.40803	101	H	8.101802	0.539483	2.349842
7	H	9.281576	1.85971	-0.86843	102	H	8.81918	-1.717	1.643751
8	H	8.672472	-0.41235	-1.62855	103	H	7.163533	-3.41024	0.947441
9	C	4.702667	2.970457	-0.69152	104	C	5.306543	1.338917	2.373688
10	C	2.537414	3.283999	-0.62457	105	C	3.545276	2.588641	2.734139
11	C	3.169598	4.480104	-0.22562	106	C	4.69489	3.339308	3.058444
12	C	1.14419	3.170613	-0.6445	107	C	2.262045	3.124389	2.880558
13	C	2.435205	5.611228	0.135282	108	C	4.604025	4.651564	3.528149
14	C	0.41918	4.291383	-0.27896	109	C	2.175925	4.419951	3.356669
15	H	0.674795	2.236925	-0.92937	110	H	1.38864	2.535635	2.62552
16	C	1.055399	5.493116	0.097489	111	C	3.328036	5.171583	3.670842
17	H	2.915012	6.533814	0.442042	112	H	5.483412	5.235338	3.777614
18	H	-0.6658	4.246129	-0.27814	113	H	1.199072	4.875889	3.483649
19	H	0.446355	6.348064	0.374453	114	H	3.211695	6.18724	4.036125
20	C	5.90896	-1.22542	-2.02088	115	C	4.310912	-2.8473	0.862866
21	C	4.213895	-2.47663	-2.62288	116	C	2.181385	-3.17112	0.481468

22	C	5.397149	-3.22844	-2.77732	117	C	2.867317	-4.37356	0.209375
23	C	2.96401	-3.01612	-2.94261	118	C	0.799776	-3.06547	0.293153
24	C	5.375427	-4.54116	-3.25251	119	C	2.198012	-5.51384	-0.23908
25	C	2.946477	-4.31561	-3.41711	120	C	0.140093	-4.19691	-0.15358
26	H	2.062353	-2.42812	-2.81695	121	H	0.288367	-2.12982	0.485533
27	C	4.131956	-5.0658	-3.56611	122	C	0.828166	-5.40127	-0.41188
28	H	6.283014	-5.12158	-3.37715	123	H	2.719133	-6.43969	-0.45604
29	H	1.996998	-4.77427	-3.67477	124	H	-0.93269	-4.15762	-0.31729
30	H	4.069042	-6.08285	-3.94041	125	H	0.269184	-6.26315	-0.76299
31	N	6.440566	-2.41473	-2.37801	126	N	4.205299	-4.13027	0.455255
32	N	4.568222	-1.24046	-2.14316	127	N	3.106911	-2.24657	0.895151
33	N	3.51855	2.371234	-0.91747	128	N	3.962382	1.355741	2.299353
34	N	4.530514	4.242698	-0.27075	129	N	5.783969	2.523978	2.812119
35	C	7.840568	-2.79876	-2.34394	130	C	5.28213	-5.09713	0.328989
36	H	8.40732	-2.2341	-3.08727	131	H	6.01076	-4.75527	-0.40723
37	H	8.248933	-2.62979	-1.34587	132	H	5.762177	-5.24971	1.297653
38	H	7.908448	-3.86036	-2.57508	133	H	4.860855	-6.04082	-0.01102
39	C	5.56728	5.201974	0.069484	134	C	7.176121	2.88692	3.010963
40	H	6.189979	4.811374	0.876104	135	H	7.615302	2.277195	3.803283
41	H	6.177508	5.422893	-0.80867	136	H	7.731495	2.75499	2.080763
42	H	5.08983	6.118238	0.410386	137	H	7.222007	3.934044	3.302965
43	N	5.621814	0.940333	-1.28265	138	N	5.129536	-0.82116	1.592188
44	Pt	3.699355	0.474591	-1.5653	139	Pt	3.185872	-0.34982	1.570486
45	C	1.833645	0.046186	-1.92093	140	C	1.283946	0.075463	1.63005
46	C	0.650948	-0.22032	-2.1137	141	C	0.080269	0.317237	1.670391
47	C	-0.74042	-0.48614	-2.19716	142	C	-1.32303	0.534201	1.674793
48	C	-1.22572	-1.78482	-2.44866	143	C	-2.20354	-0.55156	1.5033
49	C	-1.66697	0.546678	-1.95915	144	C	-1.87074	1.823746	1.833636
50	C	-2.58277	-2.05158	-2.39624	145	C	-3.56986	-0.35283	1.492507
51	H	-0.52256	-2.58301	-2.66268	146	H	-1.79909	-1.54895	1.361114
52	C	-3.02061	0.27715	-1.91841	147	C	-3.24142	2.016644	1.81837
53	H	-1.30876	1.55358	-1.77195	148	H	-1.20511	2.66944	1.975794
54	C	-3.50748	-1.03032	-2.10818	149	C	-4.12554	0.931143	1.651816
55	H	-2.94048	-3.05833	-2.59019	150	H	-4.22768	-1.19582	1.318874
56	H	-3.71637	1.07317	-1.67958	151	H	-3.64188	3.013954	1.971718
57	C	-4.93351	-1.30031	-1.92789	152	C	-5.57455	1.117725	1.630896
58	C	-5.34529	-2.47119	-1.22521	153	C	-6.41899	0.090064	2.154253
59	C	-6.6509	-3.0189	-1.36249	154	C	-7.7368	-0.11127	1.657288

60	C	-4.48077	-3.12441	-0.30311	155	C	-5.9674	-0.83968	3.132234
61	C	-7.08077	-4.07774	-0.60534	156	C	-8.51002	-1.17525	2.04113
62	H	-7.31367	-2.61994	-2.12374	157	H	-8.12331	0.55746	0.89683
63	C	-4.89935	-4.17087	0.475249	158	C	-6.73343	-1.90072	3.540194
64	H	-3.47257	-2.75029	-0.16492	159	H	-5.00114	-0.68712	3.602109
65	C	-6.22993	-4.66958	0.373947	160	C	-8.0238	-2.12948	2.97969
66	H	-8.07212	-4.47977	-0.77633	161	H	-9.48552	-1.30408	1.588611
67	H	-4.20962	-4.6002	1.191255	162	H	-6.35106	-2.56133	4.308786
68	C	-5.86664	-0.31554	-2.38042	163	C	-6.1248	2.295281	1.032539
69	C	-5.56775	0.538748	-3.47587	164	C	-5.47362	2.957771	-0.04177
70	C	-7.09396	-0.07872	-1.70897	165	C	-7.36908	2.834823	1.451596
71	C	-6.41339	1.544786	-3.86564	166	C	-6.03878	4.028854	-0.68626
72	H	-4.66257	0.365484	-4.0494	167	H	-4.52527	2.575655	-0.40333
73	C	-7.93282	0.948098	-2.05948	168	C	-7.93744	3.920136	0.834881
74	H	-7.34629	-0.68191	-0.84517	169	H	-7.8608	2.41175	2.321837
75	C	-7.61377	1.811889	-3.14557	170	C	-7.30435	4.540471	-0.28022
76	H	-6.15474	2.140661	-4.73191	171	H	-5.52068	4.466301	-1.53092
77	H	-8.83208	1.111279	-1.47784	172	H	-8.86352	4.321511	1.227518
78	N	-6.65946	-5.6664	1.168381	173	N	-8.75411	-3.20772	3.316747
79	N	-8.40763	2.849766	-3.47357	174	N	-7.88059	5.574867	-0.92251
80	C	-5.74219	-6.31972	2.085613	175	C	-8.22807	-4.19514	4.241674
81	H	-5.33483	-5.60743	2.811367	176	H	-8.12717	-3.7842	5.253422
82	H	-6.27927	-7.09449	2.630396	177	H	-8.91099	-5.04251	4.280832
83	H	-4.90918	-6.78796	1.549168	178	H	-7.24949	-4.55802	3.913158
84	C	-8.02041	-6.16093	1.066787	179	C	-10.1026	-3.37101	2.802445
85	H	-8.18541	-6.69389	0.122388	180	H	-10.1051	-3.43725	1.708581
86	H	-8.2085	-6.84925	1.889506	181	H	-10.5254	-4.29133	3.202239
87	H	-8.74067	-5.34094	1.135812	182	H	-10.7452	-2.53551	3.101817
88	C	-9.64244	3.090471	-2.74965	183	C	-9.18679	6.058145	-0.51609
89	H	-10.0642	4.039655	-3.07678	184	H	-9.54383	6.775513	-1.25402
90	H	-10.379	2.299147	-2.93484	185	H	-9.90757	5.236303	-0.46382
91	H	-9.45836	3.151318	-1.67291	186	H	-9.14895	6.553848	0.461886
92	C	-8.10392	3.669854	-4.63287	187	C	-7.16761	6.277699	-1.97282
93	H	-8.82395	4.485075	-4.6884	188	H	-7.78906	7.094995	-2.33584
94	H	-7.10152	4.103467	-4.55888	189	H	-6.22591	6.697964	-1.60188
95	H	-8.164	3.088876	-5.56112	190	H	-6.94454	5.61552	-2.81572

References

1 A. Mondal, H. Chen, L. Flämig, P. Wedi, M. van Gemmeren, *J. Am. Chem. Soc.* 2019, **141**, 18662.

2 I. Papadopoulos, J. Zirzlmeier, C. Hetzer, Y. J. Bae, M. D. Krzyaniak, M. R. Wasielewski, T. Clark, R. R. Tykwinski, D. M. Guldi, *J. Am. Chem. Soc.* 2019, **141**, 6191.

3 M. J. T. Frisch, G. W. Schlegel, H. B. Scuseria, M. A. Robb, J. R. Cheeseman, G. Scalmani, V. Barone, B. Mennucci, G. A. Petersson, H. Nakatsuji, M. Caricato, X. Li, H. P. Hratchian, A. F. Izmaylov, J. Bloino, G. Zheng, J. L. Sonnenberg, M. Hada, M. Ehara, K. Toyota, R. Fukuda, J. Hasegawa, M. Ishida, T. Nakajima, Y. Honda, O. Kitao, H. Nakai, T. Vreven, J. A. Montgomery Jr., J. E. Peralta, F. Ogliaro, M. Bearpark, J. J. Heyd, E. Brothers, K. N. Kudin, V. N. Staroverov, T. Keith, R. Kobayashi, J. Normand, K. Raghavachari, A. Rendell, J. C. Burant, S. S. Iyengar, J. Tomasi, M. Cossi, N. Rega, J. M. Millam, M. Klene, J. E. Knox, J. B. Cross, V. Bakken, C. Adamo, J. Jaramillo, R. Gomperts, R. E. Stratmann, O. Yazyev, A. J. Austin, R. Cammi, C. Pomelli, J. W. Ochterski, R. L. Martin, K. Morokuma, V. G. Zakrzewski, G. A. Voth, P. Salvador, J. J. Dannenberg, S. Dapprich, A. D. Daniels, O. Farkas, J. B. Foresman, J. V. Ortiz, J. Cioslowski, D. J. Fox, Gaussian 09, Revision D.01; Gaussian, Inc.: Wallingford, CT, 2013.

4 Y. Zhao, D. G. Truhlar, *Theor. Chem. Acc.* 2008, **120**, 215.

5 Y. Zhao, D. G. Truhlar, *Acc. Chem. Res.* 2008, **41**, 157.

6 A. V. Marenich, C. J. Cramer, D. G. Truhlar, *J. Phys. Chem. B* 2009, **113**, 6378.

7 R. Bauernschmitt, R. Ahlrichs, *Chem. Phys. Lett.* 1996, **256**, 454.

8 M. E. Casida, C. Jamorski, K. C. Casida, D. R. Salahub, *J. Chem. Phys.* 1998, **108**, 4439.

9 R. E. Stratmann, G. E. Scuseria, M. J. Frisch, *J. Chem. Phys.* 1998, **109**, 8218.

10 E. R. Johnson, S. Keinan, P. Mori-Sánchez, J. Contreras-García, A. J. Cohen, W. Yang, *J. Am. Chem. Soc.* 2010, **132**, 6498.

11 J. Contreras-García, E. R. Johnson, S. Keinan, R. Chaudret, J.-P. Piquemal, D. N. Beratan, W. Yang, *J. Chem. Theory Comput.* 2011, **7**, 625.

12 W. Humphrey, A. Dalke, K. Schulten, *J. Mol. Graphics,* 1996, **14**, 33.

13 D. Andrae, U. Häußermann, M. Dolg, H. Stoll, H. Preuß, *Theor. Chim. Acta.* 1990, **77**, 123.

14 M. Dolg, P. Pyykkö, N. Runeberg, *Inorg. Chem.* 1996, **35**, 7450.

15 W. J. Hehre, R. Ditchfield, J. A. Pople, *J. Chem. Phys.* 1972, **56**, 2257.

16 P. C. Hariharan, J. A. Pople, *Theor. Chim. Acta.* 1973, **28**, 213.

17 J. D. Dill, J. A. Pople, *J. Chem. Phys.* 1975, **62**, 2921.

18 Y. Jiang, Y. Wang, N. Ma, Z. Wang, M. Smet, X. Zhang, *Langmuir* 2007, **23**, 4029.